

Review

# Forever Chemicals, Per- and Polyfluoroalkyl Substances (PFAS), in Lubrication

Darrius Dias <sup>1,†</sup> , Jake Bons <sup>1,†</sup>, Abhishek Kumar <sup>1,†</sup> , M. Humaun Kabir <sup>2,†</sup> and Hong Liang <sup>1,2,\*</sup> 

<sup>1</sup> J. Mike Walker '66 Department of Mechanical Engineering, Texas A&M University, College Station, TX 77843-3123, USA; djdias2000@tamu.edu (D.D.); jakebons@tamu.edu (J.B.); akumar71@tamu.edu (A.K.)

<sup>2</sup> Department of Materials Science and Engineering, Texas A&M University, College Station, TX 77843-3127, USA; mkhumaun@tamu.edu

\* Correspondence: hliang@tamu.edu

† These authors contributed equally to this work.

**Abstract:** Per- and polyfluoroalkyl substances (PFAS), also known as forever chemicals, exhibit exceptional chemical stability and resistance to environmental degradation thanks to their strong C-F bonds and nonpolar nature. However, their widespread use and persistence have a devastating impact on the environment. This review examines the roles of PFAS in tribological applications, specifically in lubricants and lubricating systems. This article focuses on conventional and advanced lubricants, including ionic liquids (ILs) and their use in modern automotive vehicles. The objective of this paper is to provide a comprehensive overview of the adverse impacts of PFAS whilst acknowledging their outstanding performance in surface coatings, composite materials, and as additives in oils and greases. The pathways through which PFAS are introduced into the environment via lubricating systems such as in seals and O-rings are identified, alongside their subsequent dispersion routes and the interfaces across which they interact. Furthermore, we examine the toxicological implications of PFAS exposure on terrestrial and aquatic life forms, including plants, animals, and humans, along with the ecological consequences of bioaccumulation and biomagnification across trophic levels and ecosystems. This article ends with potential remediation strategies for PFAS use, including advanced treatment technologies, biodegradation, recovery and recycling methods, and the search for more environmentally benign alternatives.



**Citation:** Dias, D.; Bons, J.; Kumar, A.; Kabir, M.H.; Liang, H. Forever Chemicals, Per- and Polyfluoroalkyl Substances (PFAS), in Lubrication. *Lubricants* **2024**, *12*, 114. <https://doi.org/10.3390/lubricants12040114>

Received: 6 March 2024

Revised: 25 March 2024

Accepted: 27 March 2024

Published: 29 March 2024



**Copyright:** © 2024 by the authors. Licensee MDPI, Basel, Switzerland. This article is an open access article distributed under the terms and conditions of the Creative Commons Attribution (CC BY) license (<https://creativecommons.org/licenses/by/4.0/>).

**Keywords:** forever chemicals; PFAS; tribology; coatings; lubricants; materials

## 1. Introduction

Per- and polyfluoroalkyl substances (PFAS) is a term used to describe a class of synthetic compounds that has seen widespread but controversial use over the past century in almost every recognized industry. PFAS is a modern term that describes substances once known as perfluorinated chemicals (PFCs) [1]. They are colloquially known as “forever chemicals” in news and media, a moniker was first coined by Joseph Allen at the Harvard T.H. Chan School of Public Health due to the extensive half-lives of these materials from various degradation studies [2–4]. In 1862, Alexander Borodin was credited with carrying out the earliest nucleophilic replacement using fluoride. This work was followed up in 1926 by French chemists Lebeau and Damiens who isolated carbon tetrafluoride from a reaction using fluorine and charcoal [5], and in 1934 Fritz Schloffer and Otto Scherer were able to polymerize polychlorotrifluoroethylene (PCTFE) [6]—an early example of PFAS now known as Neoflon<sup>®</sup>. Modern-day PFAS can trace its beginnings to 1939, where Roy J. Plunkett filed a patent for the discovery of tetrafluoroethylene polymers while working for DuPont de Nemours, citing the need for satisfactory materials to safely handle corrosive agents [7]. The substance was synthesized on a large scale for nuclear weapon production during World War II as a material in contact with uranium hexafluoride (UF<sub>6</sub>) [5].

Polytetrafluoroethylene (PTFE) was later trademarked by DuPont as Teflon® and was a commercial success.

PFAS has now been widely applied in products such as adhesives, ammunition, cleaning products, construction, cosmetics, electronics, fertilizers, firefighting foam, manufacturing, medical devices, mining, oil and gas, paints, pesticides, propellants, refrigerants, semiconductors, textiles, transportation, varnish, and much more [8]. Several classes of these synthetic materials and substances have attracted interest in the field of tribology due to their distinctive and advantageous properties [1,8,9]. These compounds, notable for their oil- and water-repellent characteristics and high thermal stability, have effectively reduced friction and wear in diverse mechanical systems. A popular use of PFAS in tribological applications is the utilization of PTFE in coatings and lubricants, renowned for its lubricity, resilience at high temperatures, and resistance to chemical attacks [10–12]. In the automotive sector, PFAS has seen significant use in the development of lubricants, engine oils, and hydraulic fluids [13–15]. It plays a crucial role in supplying essential features such as antiwear, anticorrosion, and antifoaming capabilities. These oils frequently include additives such as organophosphate esters (OPEs), which are commonly present in amounts ranging from 0.1 to 30 percent by volume [16,17]. It is worth mentioning that the annual demand for vehicle lubricating oils in the United States is approximately 2.4 billion gallons [18].

In recent years, the use of PFAS has fallen under increasing scrutiny. Although PFAS provides several indisputable advantages, concerns over its environmental and health effects are arising in current industrial practices and government regulations [1,9]. PFAS exhibit a concerning level of persistence in the environment, as they are resistant to natural decomposition mechanisms. The noble nature of these substances, along with their capacity to accumulate in the bodies of living organisms, presents ecological challenges. Typical tribological applications, such as coatings, oils, and commercial or specialized lubricants, lead to the removal of PFAS particles from the original system by wear, vaporization, or other mass loss. Humans are exposed to PFAS through lubricant and environmental interfaces via inhalation, ingestion, or direct contact. A simple depiction of this exposure is illustrated in Figure 1. PFAS chemicals contribute to environmental pollution by leaching into the soil surrounding landfills and by contaminating surface and ground water through the release of airborne particles and precipitation. These pollutants and contaminants directly or indirectly affect plants, animals, and humans. Biomagnification increases the concentration of PFAS in the human body, which could lead to potentially fatal health issues [19]. Ongoing research and development endeavors are being directed towards discovering safer substitutes and to establish conscientious methods for their utilization.

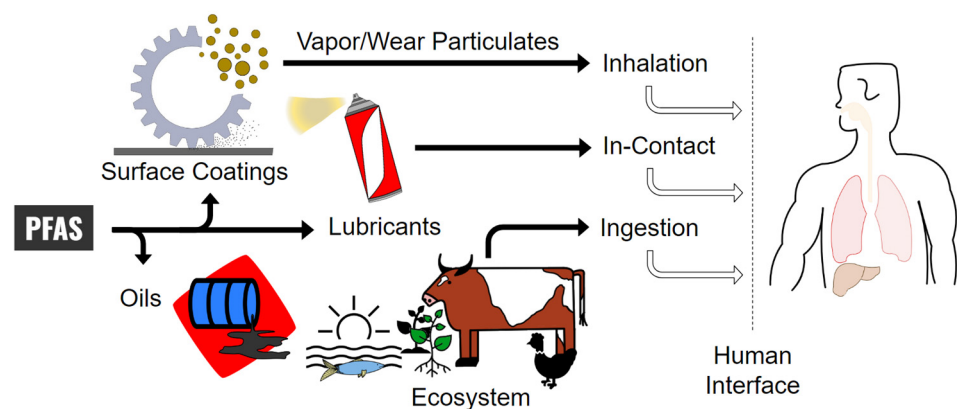


**Figure 1.** Illustration of the impact of PFAS on the environment and humans through tribological applications.

This paper aims to offer an objective review of PFAS while exploring its multifaceted role in tribological applications. Lubrication referred to in this work includes lubricants

and lubricating systems. The utilization of these substances is surveyed by examining the mechanisms by which PFAS are introduced into the environment after their use in lubricant, alongside their subsequent dispersion pathways, evaluating the potential harm they do to the environment, highlighting the toxicological implications of PFAS exposure on terrestrial and aquatic life forms, and investigating the regulatory framework that governs their applications. The characteristics of PFAS are outlined in Section 2, including their classification and lubrication mechanisms, while further exploring their specific uses in lubrication in Section 3, and assessing the environmental and health consequences in Section 4. Furthermore, Section 5 evaluates waste management options for PFAS and explores potential alternatives. A concluding note to this comprehensive review summarizes the current status and future possibilities of PFAS in tribological applications. To successfully negotiate this challenging environment, it is essential to comprehend both the benefits and concerns related to the use of PFAS.

## 2. PFAS in Lubrication

### 2.1. Classifications

PFAS compounds are distinguished by their carbon backbone, which is extensively saturated with fluorine atoms and typically contains functional groups such as carboxylic acid, sulfonic acid, or amine [8]. Perfluoroalkyls are defined by the complete substitution of hydrogen atoms linked to carbon with fluorine, except in cases where this substitution would modify any functional groups, whereas polyfluoroalkyls are compounds in which just a portion of their hydrogen atoms are substituted with fluorine, containing the perfluoroalkyl molecule  $C_nF_{2n+1}$  [1].

The remarkable stability of the C-F bond is attributed to fluorine's high electronegativity combined with the atom's reasonably small size [20]. The intrinsic stability of PFAS compounds makes them resilient to degradation in various biological and environmental conditions [21]. Although biodegradation typically relies on enzymes to break down organic materials, many organisms and enzymes struggle to sever PFAS's C-F bonds, hindering natural biodegradation [22,23]. PFAS molecules are typically long and hydrophobic, which makes it difficult for microorganisms to break down [23]. Moreover, the lengthy, hydrophobic nature of PFAS molecules, coupled with their chemical inactivity, further challenges their breakdown [24,25]. PFAS compounds exhibit high thermal stability and exceptional acid degradation resistance primarily due to their strong C-F bonds [26,27]. The strength of the C-F bond, superior to the C-H bonds in many organic molecules, prevents acids from easily attacking or forming strong interactions, thanks to the nonpolar nature of these materials and the steric hindrance offered by the bulky fluorine atoms. This combination of chemical resistance and physical barrier makes PFAS materials highly durable in aggressive chemical environments.

PFAS compounds are primarily classified into polymer and nonpolymer types, each with distinct molecular structures and applications [1,28], which are illustrated in Figure 2. Polymeric PFAS features extensive chains of perfluorinated monomeric units and is subdivided into fluoropolymers, sidechain fluorinated polymers, and perfluoropolyethers. Notably, fluoropolymers such as PTFE are used in creating nonstick coatings such as Teflon [29–31]. These polymers are also prevalent in various industries due to their resistance to heat and chemical agents, serving in nonstick cookware, electrical insulation, and industrial components such as seals and gaskets [32,33]. Conversely, nonpolymeric PFAS comprise smaller molecules without long repeating units. They include subfamilies such as perfluoroalkyl acid (PFAA), perfluoroalkyl ether (PFPE), fluorotelomer (FT), and perfluoroalkane sulfonyl fluoride (PASf) [34]. Their applications are equally diverse, ranging from chrome plating and hydraulic fluids [35,36] to sectors such as electronics and semiconductors [37]. Additionally, compounds such as perfluorosulfonic acid (PFSA) and perfluorocarboxylic acids (PFCA) are integral in firefighting foams [38,39], highlighting the widespread utility of nonpolymeric PFAS in various commercial and industrial settings.

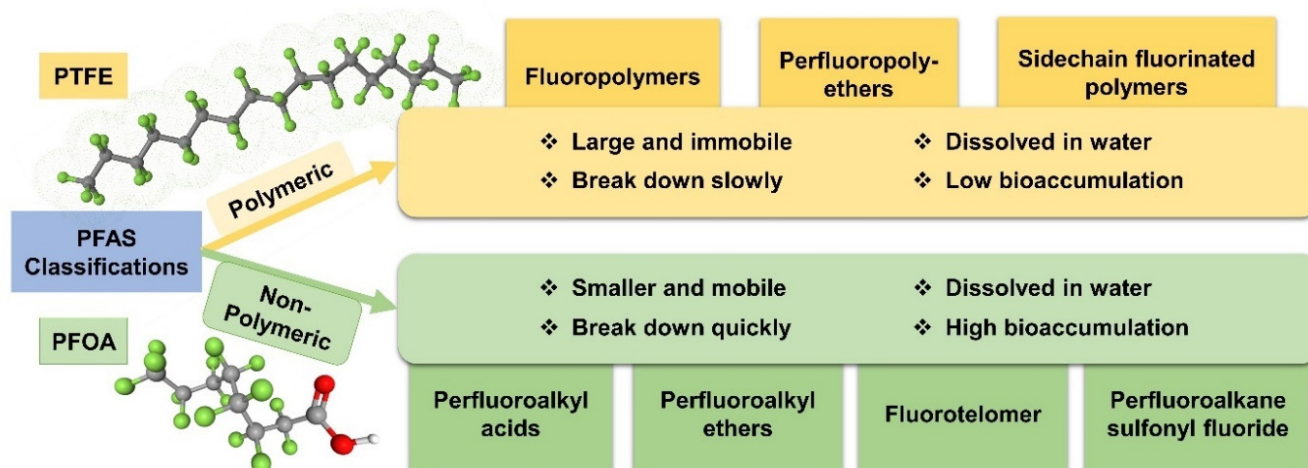


Figure 2. Classifications of PFAS and their primary properties.

## 2.2. Manufacturing Techniques

The manufacturing of per- and polyfluoroalkyl substances (PFAS) follows a systematic process that transitions from monomer synthesis to the application of the final product as a coating. Electrochemical fluorination (ECF) and telomerization stand as the foundational methods for producing PFAS [1]. ECF, historically employed by companies until 2001, involves organic molecules and fluorine gas undergoing electrolysis in a hydrogen fluoride medium. Despite its efficacy in fluorinating organic compounds, ECF can lead to a variety of byproducts, some of which may be environmentally concerning [1,4]. Telomerization, a more contemporary method developed in the 1970s, has been favored for its specificity in crafting PFAS chains and is perceived to be less polluting. It achieves this by initiating a reaction between short-chain hydrocarbons and fluorinated telomers, producing a series of perfluoroalkyl iodides with extended chains [1,40].

Incorporating the advanced manufacturing techniques of PFAS alongside the foundational methods enhances the scope of their application and functional properties. Figure 3 shows the flowchart of developing PFAS from their monomer. Initially, monomers such as tetrafluoroethylene (TFE) and vinylidene fluoride (VDF) are derived from basic chemical compounds [41,42]. TFE is obtained from fluorspar ( $\text{CaF}_2$ ), sulfuric acid ( $\text{H}_2\text{SO}_4$ ), and chloroform ( $\text{CHCl}_3$ ), while VDF is produced using 1-chloro-1,1-difluoroethane ( $\text{CHClF}_2$ ) and hydrofluoric acid (HF). Subsequently, these monomers undergo polymerization to form PFAS polymers. Fine powder forms of PFAS are typically achieved through solution or emulsion polymerization, a process characterized by the creation of polymer chains within a liquid medium. The alternative resin form of PFAS is produced through gamma-irradiation, which involves using high-energy radiation to initiate the polymerization reaction [43]. For paste forms, PFAS polymers are subjected to extreme extrusion pressure, which aligns the polymer chains and imparts the necessary viscosity and texture [44]. Granular forms of PFAS are created by sintering polymer powders with fillers, a process that involves heating the powder below its melting point to create solid particles [45].

Advancing to nanocomposites, high shear mixing is essential to prevent the agglomeration of nanoparticles within the PFAS polymer matrix, ensuring even distribution [42,46]. Ultrasonication further aids in breaking up clusters, allowing for more uniform dispersion of nanoparticles [47]. Solution blending techniques involve dissolving the polymer and nanoparticles in a solvent to achieve a homogenous mixture, while melt blending requires mixing and heating until the polymer melts, allowing for the integration of nanoparticles into the viscous fluid [48,49]. The final stage involves applying the PFAS polymers as coatings, utilizing a range of techniques based on the application requirements. Spin coating is used to achieve a uniform thickness, particularly valuable in applications demanding consistent coverage across surfaces [50,51]. Electrospinning is harnessed to

produce ultrafine fibers, leveraging the high surface area of nanofibers for applications such as filtration [52–54]. Spray coating is adept at covering complex shapes and vast areas, while electrostatic powder coating is known for its ability to provide a uniform, solid coat, essential for durable and protective finishes [55–57].

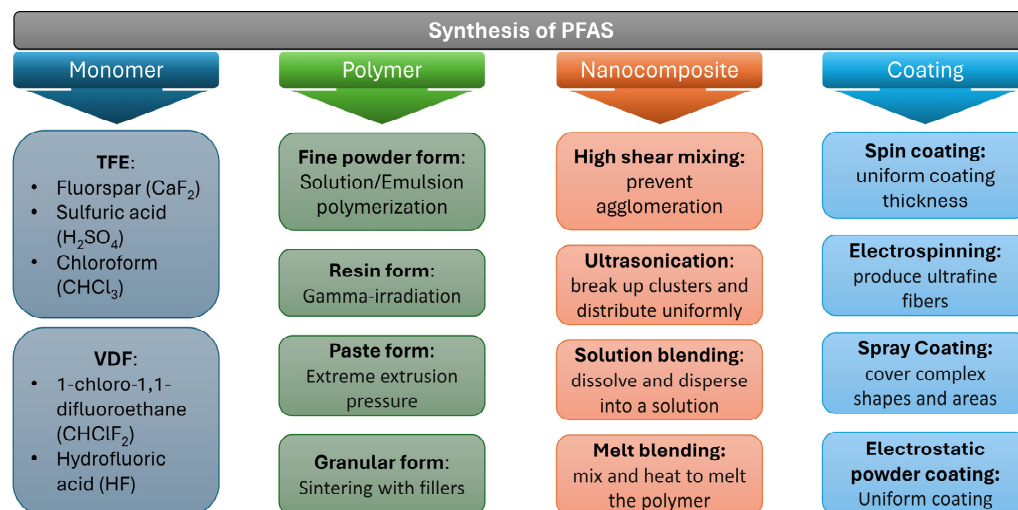


**Figure 3.** Synthesis routes of PFAS.

Each step in the manufacturing process of PFAS polymers is critical, from the initial synthesis of monomers to the development of advanced coatings. The versatility of PFAS, when coupled with the sophisticated methods of polymerization and coating application, underscores the wide range of applications and superior performance attributes these materials can offer.

### 2.3. Lubrication Mechanisms of PFAS

PFAS have found widespread use in tribological applications due to their distinctive characteristics, including lubricity, hydrophobicity, low surface energy, chemical inertness, and high thermal stability [1,9]. They are commonly used in circumstances where alternative chemicals are unable to fulfill the required performance standards [1] and meet strict performance requirements, while lesser quantities of PFAS can yield the same level of efficiency as greater quantities of nonfluorinated compounds [9]. Additionally, the intrinsic hydrophobic and oleophobic properties of the perfluorocarbon constituents of PFAS render them exceptionally effective in their functions as surfactants or agents for protecting surfaces [58]. Evaluating the levels of PFAS in this particular category of products will offer insightful data about the origins of these substances in the environment [59].

A few possible mechanisms for PFAS to achieve high tribological performance are illustrated in Figure 4. The tetrahedral structure of the molecules generates hydrophobicity, resulting in a nonadhesive behavior that effectively reduces the COF value [12,24,60]. The inherent hydrophobicity provides a low surface energy, which reduces the adhesive bonds between the surfaces and can reduce the coefficient of friction. In addition, the presence of strong C-F bonds enhances its efficacy in countering frictional stresses. Moreover, the material's inherent smoothness lessens direct asperity contact, minimizing surface wear and ensuring the longevity of contact surfaces. The molecular architecture of PFAS plays a pivotal role in defining their tribological behavior, particularly influencing their capacity to exhibit low friction coefficients. PFAS molecules consist of a lengthy hydrocarbon chain that is arranged in a parallel manner. This tight packing within the crystalline regions results in a remarkably smooth surface at the microscopic level, reducing mechanical interlocking and enabling effortless sliding between contacting surfaces. The orderly and parallel nature of these chains reduces intermolecular entanglement, thereby providing a stable, low-friction interface. The combined effects of the crystalline structure in PTFE

and the parallel alignment in PFAS highlight the significance of molecular configuration in determining the frictional performance of these materials.

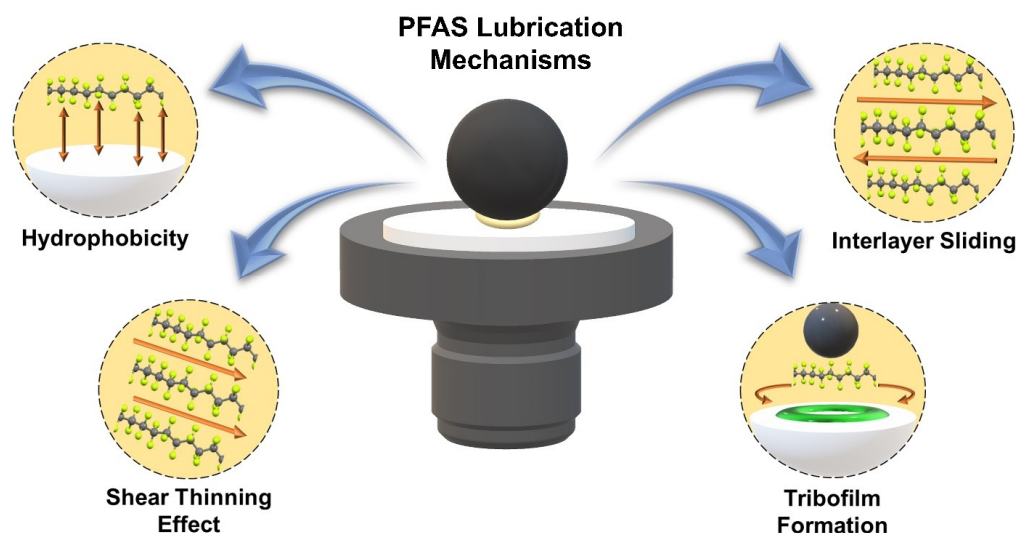


**Figure 4.** Lubrication mechanisms of PFAS materials.

Furthermore, the high performance in lubrication systems of PFAS also depends on its shear-thinning effects and formation of tribofilms [12,61]. This rheological property results in a decrease in viscosity with an increase in fluid shear rate. PFAS materials consist of long molecular chains adorned with fluorine atoms, which exhibit a range of conformations due to their carbon-carbon bond rotations. In scenarios of low shear stress, these molecules tend to entangle, leading to a high viscosity and substantial internal resistance to flow. However, under increased shear rates, the molecular chains align in the direction of the flow. This realignment reduces entanglement and facilitates easier motion of the molecules relative to each other, resulting in a notable decrease in viscosity. PTFE is able to effectively reduce friction during sliding contact by forming a protective layer. As PTFE slides, it transfers small particles onto the contacting surfaces through adhesive wear. The wear debris can then be compressed to form a tribofilm that helps lower the friction.

#### 2.4. Applications of PFAS in Modern Automobiles

PFAS has been widely used in high-performance mechanical systems such as vehicle combustion engines, electric motors, batteries and charging systems, power electronics, thermal management systems, and many others. Components in modern vehicles are subject to challenging conditions such as mechanical loading, cyclic stresses, and high temperatures [37]. Electric vehicles (EVs) have a lower number of components compared to their internal combustion engine (ICE) counterparts, and the performance demands on these components are greater due to the harsher operating conditions. These design requirements mean that stable PFAS products are prime candidates for use in such applications, but it also raise challenges when it comes to replacing PFAS with suitable and sustainable alternatives in the manufacturing process [37].

A majority of ICE vehicles contain several PFAS materials applied to key areas at every level of their design from the “cradle to the grave”. For example, PTFE tubing can withstand temperature fluctuations of various circulating fluids used for thermal management or lubrication. These tubes are sometimes filled with various filler additives to improve their performance. Shrink sleeves play an important role in maintaining sealed insulation of power electronic systems—especially important in increasingly electrified components experiencing ever-increasing voltages. These components account for ever-increasing additions to e-waste generated from modern vehicles, which raise their handling, emissions, and exposure concerns [62]. Encapsulated probes and thermowells comprising

PFAS materials are inserted into ICE spaces to monitor mileage performance and efficiency. PFAS are even used during vehicle emissions testing in the form of PVF (Tedlar®) and or FEP gas sampling bags. These low-cost, low-permeation sample holders are used to inertly store emission samples from tested vehicles to analyze whether they meet regulatory standards. Vehicle tires are also known to contribute to about 4.8–12.7 million tons of microplastic waste, which is compounded by additional drivers entering roads year after year, and higher-performance vehicles being added to the market [63]. Lastly, the disposal of modern automobiles in recovery and salvage yards has led to municipal wastewater pollution concerns from runoff, exposure, erosion, and sedimentation. Automotive and metal recovery yards can account for up to 75% of PFAS site contamination and up to 2000 g/yr in PFAS mass flux leachate [64]. EPA regulations under the National Pollutant Discharge Elimination System (NPDES) were developed in 1990 to control stormwater discharges associated with industrial activity by issuing stormwater permits to control runoff from industrial facilities processing automobile waste.

The functionality of PFAS materials plays a crucial part in the ongoing energy transition towards e-mobility, where battery electric vehicles (BEVs) and fuel cell electric vehicles (FCEVs) have emerged as the two current front runners. EV traction batteries contain PVDF binders for a protective cathode coating [65–67]. Electrolytes are enhanced with fluorobenzene and fluoroethylene carbonate (FEC) to extend battery cell longevity by creating a barrier on anodes to inhibit interaction with the electrolyte [68,69]. PFAS have been used in fuel cells, making up materials in the polymer electrolyte membranes, gas diffusion layers, electrodes, and coolants [70,71]. Polymers such as PTFE, fluorinated ethylene propylene (FEP), and fluoroelastomers (FKM) can withstand the acidic and high-temperature conditions at the membrane/catalyst in the fuel cell, finding use in rubber seals and housing materials [72]. Onboard power electronics contain PFAS in semiconductors, liquid crystals, diaphragms, and coatings, which are crucial to autonomous driving modules [73]. Textiles and woven membranes made of PFAS can help extend component lifetimes via their hydrophilic and antiwear properties, but their disposal process has also been linked to further PFAS emissions [73,74]. Figure 5 summarizes the use of PFAS in various automotive components.

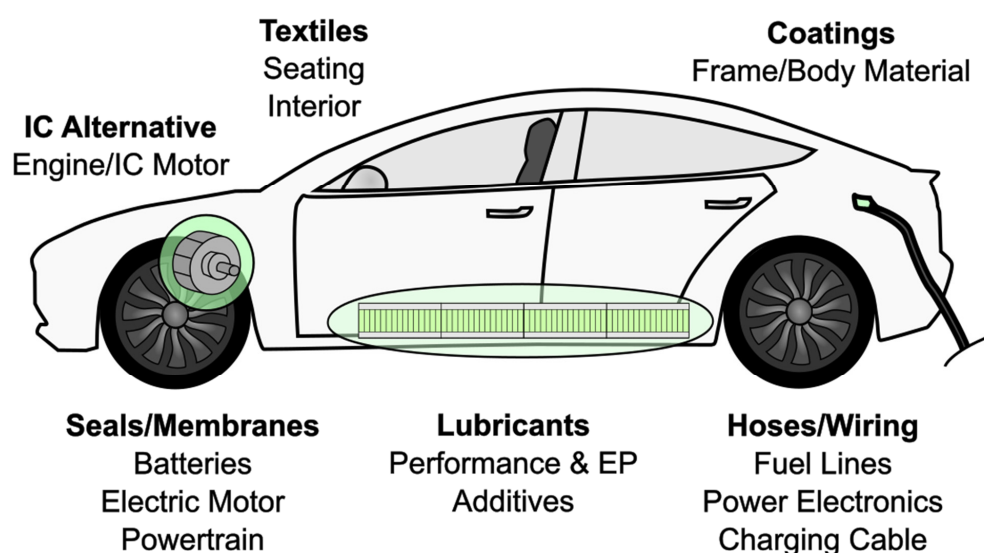


**Figure 5.** PFAS in various parts of automotive components.

### 2.5. PFAS in Coatings and Composite Materials

Advancements in coatings have made them suitable for a wide range of applications. PFAS materials such as PTFE and PVDF exhibit several unique properties [46,75,76] making them the two primary PFAS coatings in common use. Thick PTFE coatings, ranging in thickness from 5 to 100  $\mu\text{m}$  for bearings, 32.5 to 45  $\mu\text{m}$  for cookware, and 20 to 30  $\mu\text{m}$  for air

conditioner compressors, have become essential in various industries, presenting a viable alternative to traditional lubricants [77]. Meanwhile, PVDF, a highly nonreactive thermoplastic polymer, is recognized for its high thermal stability up to 175 °C [78]. Its versatility has seen its application across various sectors including piping products, insulators in premium wiring, binder material in composite electrodes for making lithium-ion batteries, and components in the pharmaceutical and food processing industries. Additionally, PVDF's unique crystallization phases make it an invaluable material in biomedicine, and in piezoelectric and pyroelectric applications. The combination of PTFE and PVDF coatings offers tailored solutions across a wide spectrum of industrial and technological applications.

### 2.5.1. PTFE Coatings

Polytetrafluoroethylene (PTFE), commercially recognized as Teflon, is a fluoropolymer derived from polymerizing tetrafluoroethylene, showcasing a semicrystalline nature due to its robust C-F bonds, which impart a high molecular weight and nonreactivity with other substances [79]. Its utility spans across diverse sectors owing to its exceptional properties.

PTFE finds applications in lubrication systems, including bearings and gears, due to its mechanical robustness [42]. Its outstanding dielectric properties make it a preferred choice for insulating materials in the electrical industry, such as cable coatings and components for printed circuit boards [80,81]. The medical field benefits from PTFE's inertness, employing it in the manufacturing of implants and stents, and for coating biomedical instruments [82,83]. Aerospace technology leverages PTFE for its ability to withstand extreme temperatures and vacuum conditions, applying it in coatings and as a solid lubricant for enhanced cryogenic tribology [84]. The defense sector utilizes PTFE in various capacities, from marine coatings to aircraft seals, highlighting its versatility. In the automotive industry, PTFE's low surface energy ensures effective lubrication, mitigating heat and damage from friction [84]. The food processing industry appreciates PTFE for its nonstick properties and chemical inertness, making it essential for hygienic production lines, from cookware to conveyor belts [85,86]. Moreover, its thermal stability and resistance to chemical attacks make PTFE indispensable in petrochemical and chemical processing plants [82,83]. Additionally, PTFE porous membranes serve critical roles in separation and filtration processes, including desalination and wastewater recycling, due to their durability and performance under challenging conditions [87]. Finally, its electrical insulating capabilities are utilized in a wide array of electrical components and electrostatic transducers, underpinning PTFE's integral role in modern technology and industry [88].

PTFE coatings possess unique tribological characteristics and can be applied in conjunction with several substrates to obtain synergistic properties. Table 1 highlights the various PTFE coatings with their tribological performance. For example, PTFE can provide low friction and improved durability when integrated with microarc oxidized (MAO)  $\text{Al}_2\text{O}_3$  [15]. The  $\text{Al}_2\text{O}_3$ /PTFE coating is a multilayered design, including a dense inner ceramic layer, a porous outer layer, and a top layer of PTFE. As PTFE fills in the ceramic coating's asperities, the surface roughness and porosity are reduced. Under friction, the PTFE layer forms a protective film, reducing the abrasive effect of debris and enhancing the overall tribological characteristics. This coating merges the benefits of MAO and PTFE, offering improved wear resistance and friction reduction for aluminum alloys.

Another study examined the tribological characteristics of PTFE and polydopamine (PDA) coatings, each about  $45 \pm 2 \mu\text{m}$  thick when applied to a cast iron substrate under oil-lubricated conditions [77]. Typically, PTFE coatings exhibit low adhesion to metal surfaces due to their nonstick nature, leading to high wear rates under friction. However, incorporating PDA into PTFE notably boosted the bonding to the cast iron base and enhanced its longevity. The PTFE coating's COF in oil-lubricated conditions was 0.045, which was 62.5% lower compared to dry conditions. The enhanced efficiency of the PDA + PTFE coating with oil lubrication is linked to the nanoscale mechanical characteristics and the strong intermolecular cross-linking between PTFE and PDA.

**Table 1.** Summary of tribological performance for various PTFE coatings.

Substrate	Coating	Thickness ( $\mu\text{m}$ )	Test Parameters	Performance	Refs
Aluminum	$\text{Al}_2\text{O}_3 + \text{PTFE}$	33	GCr15 Steel Ball $\varnothing = 15 \text{ mm}$ Force = 2 N RPM = 150 rpm	$\mu = 0.13$	[15]
7050 Aluminum Alloy	PTFE/PMMA	13.3	GCr15 Steel $\varnothing = 4.68 \text{ mm}$ Load = 3 N Speed = 8.4 mm/s	$\mu = 0.069$ $\Delta W = 1.04 \times 10^{-6} \text{ mm}^3/\text{N m}$	[89]
60 NiTi	PDA + PTFE	1.3	$\text{Si}_3\text{N}_4$ Ball $\varnothing = 6.35 \text{ mm}$ Load = 2 N Speed = 10 mm/s	$\mu = 0.096$	[90]
Cast Iron	PDA + PTFE	45	Chrome-Steel Ball Load = 10 N Speed = 10 mm/s	$\mu = 0.05$	[77]
Gray Cast Iron	Pyrrolidone + PTFE	20	52100 Steel Wrist Pins $\varnothing = 8 \text{ mm}$ Load = 445 N Speed = 0.22 m/s	$\mu = 0.043$ $W = 1.23 \times 10^{-6} \text{ mm}^3/\text{N m}$	[10]
	$\text{MoS}_2 + \text{PTFE}$	20		$\mu = 0.044$ $W = 3.76 \times 10^{-7} \text{ mm}^3/\text{N m}$	

Encapsulating PTFE with a polymethylmethacrylate (PMMA) shell improved its wear resistance and lubrication properties during reciprocating dry friction [89]. The findings showed that the COF of the PTFE coating reduced from 0.08 to 0.07, and the wear rate dropped dramatically from  $232 \times 10^{-6} \text{ mm}^3/\text{Nm}$  to  $1 \times 10^{-6} \text{ mm}^3/\text{Nm}$ . This enhancement of the performance is attributed to the PMMA modification increasing the strength and modulus of the material. In a comparative analysis, PTFE-based coatings demonstrated superior performance to PEEK-based coatings under both unidirectional and oscillatory motion conditions in compressors [10]. Notably, PTFE coatings combined with pyrrolidone exhibited the most effective friction reduction, achieving a friction coefficient of 0.043 in unidirectional tests. Furthermore, PTFE coatings modified with  $\text{MoS}_2$  were found to have enhanced wear resistance, evidenced by a notably low wear rate of  $3.76 \times 10^{-7} \text{ mm}^3/\text{Nm}$  [10]. This suggests that the specific blending of PTFE with pyrrolidone and  $\text{MoS}_2$  significantly improves both the frictional and wear-resistant properties of the coatings in various compressor applications.

### 2.5.2. PVDF Coatings

Another popularly used PFAS coating is PVDF which has been widely used in small-scale lubrication systems. It is a semicrystalline polymer widely recognized for its piezoelectric properties, making it a popular choice for use in micro-electromechanical systems (MEMS) and nano-electromechanical systems (NEMS) [91,92]. PVDF's unit monomer,  $\text{CH}_2\text{-CF}_2$ , exhibits a dipole due to the positively polarized fluoride side and the negatively polarized hydrogen side [93]. PVDF typically exists in  $\alpha$  and  $\beta$  phases, the aligned dipoles of the  $\beta$ -phase are essential for enhancing both its mechanical and electrical properties through a process called poling.

PVDF has garnered significant attention across various industries due to its remarkable properties and versatility. With excellent thermal stability, resistance to deformation under stress, and high crystallinity, PVDF excels as a coating material in demanding environments. Its low permeability to gases and liquids, alongside robust resistance to mechanical and corrosive damage, makes it ideal for protective applications in the chemical and petrochemical

sectors, where it serves infiltration and as a material resistant to aggressive substances [94]. The automotive industry utilizes PVDF in laminating films for exterior decoration, offering durability and resistance to environmental damage. The aerospace and aviation industries benefit from PVDF's thermal and corrosion resistance for parts such as seals and gaskets, and its dielectric properties are leveraged in electronics for wire insulation and as a dielectric in capacitors [95,96]. Notably, its piezoelectric capabilities have spurred innovation in sensor technology, offering advantages in weight and sensitivity over traditional materials [96,97]. In construction and architectural applications, PVDF coatings protect against erosion, corrosion, and weather, enhancing the longevity and aesthetic of buildings [98]. In the field of energy, particularly in nuclear power engineering, PVDF's resistance to high temperatures and radiation positions it as a key material for handling nuclear waste and in constructing components exposed to harsh conditions [79]. PVDF's unique blend of properties underpins its widespread adoption in applications demanding high performance and reliability.

The application of an external electric field to a poled PVDF aligns its dipoles upwards, thus increasing the generated adhesive force which can be measured using the tip of an atomic force microscope (AFM) [93]. Moreover, the presence of a lubricant film reduces friction and wear on the lubricated poled PVDF by acting as a fluid bearing, smoothing the movement of the AFM tip. Interestingly, while the coefficient of friction increases with the electric field on unlubricated poled PVDF, it remains unchanged on lubricated poled PVDF. This stability is due to the lubricant film preventing direct contact between the AFM tip and the PVDF surface, facilitating smoother tip movement. Furthermore, nanoscale wear studies using a diamond-tipped AFM revealed that the wear depth on lubricated poled PVDF is consistently lower than on its unlubricated counterpart. This reduced wear is attributed to the lubricant film, which minimizes contact and consequent wear between the AFM tip and the PVDF surface. These findings underscore the importance of lubrication in preserving the integrity of PVDF surfaces, particularly in applications of electric vehicles involving electric fields and mechanical stress [93].

The tunability of PVDF performance through nanoparticle incorporation, as shown in Table 2, including materials such as MoS<sub>2</sub>, ZnO, and graphene, represents a significant advancement in applying the PFAS material as a lubricant coating [99,100]. For example, the integration of 2 wt.% MoS<sub>2</sub> nanotubes has been demonstrated to decrease the friction coefficient from 0.4 to 0.1, a reduction attributed to the suppression of the  $\alpha$ -phase within the polymer matrix [99]. Furthermore, composite formulations combining graphene, ZnO, and PVDF have been reported to achieve very low friction coefficients, reaching a minimum value as low as 0.08 [100]. These findings underscore the potential of nanoparticles for enhancing the performance of PVDF, which could have wide-ranging applications in advanced material systems and technologies.

**Table 2.** Summary of tribological performance for various PVDF coating.

Substrate	Coating	Thickness ( $\mu\text{m}$ )	Test Parameters	Performance	Refs
Aluminum	40 wt.% Graphene Nanoplatelet + PVDF	15–20	AISI52100 Steel Ball $\varnothing = 9.5 \text{ mm}$ Load = 5 N Speed = 24 mm/s	$\mu = 0.10$	[101]
AISI 316	2 wt.% of MoS <sub>2</sub> + PVDF	-	AISI 316 Stainless steel $\varnothing = 6 \text{ mm}$ Load = 223 g Speed = 5 mm/s	$\mu = 0.10$	[99]
Stainless Steel	85.5 wt. % Graphene + 9.5 wt.%. Zinc Oxide + 5 wt.% PVDF	10	Stainless Steel ball $\varnothing = 6.3 \text{ mm}$ Load = 10 N	$\mu = 0.08$	[100]

### 2.5.3. Composite Materials

PFAS demonstrates its versatility not only in coatings, but also in composite materials where it finds a range of valuable applications. Table 3 presents a comprehensive overview of the tribological performance, highlighting the wear resistance and frictional properties of various PFAS composites under different operational conditions.

**Table 3.** Summary of tribological performance for various PFAS composites.

Composite	Test Parameters	Performance	Refs
5.0% MgO + PVDF	Load = 3 N Speed = 10 mm/s	$\mu = 0.091$ $W = 1.2 \times 10^{-5}$ $\text{mm}^3/\text{N m}$	[102]
10 wt.% Carbon Nanorod + PVDF	Stainless Steel Ball $\varnothing = 6$ mm Load = 3 N Speed = 10 mm/s	$\mu = 0.03$ $W = 3.70 \times 10^{-5}$ $\text{mm}^3/\text{N m}$	[103]
50 wt.% Polyamide 66 + PVDF	52100 Steel Ring Load = 200 N Speed = 0.43 m/s	$\mu = 0.49$ $W = 1.5 \times 10^{-5}$ $\text{mm}^3/\text{N m}$	[104]
20 wt.% PAO/PSF + Recycled PVDF	GCr15 Steel Ball $\varnothing = 6$ mm Load = 10 N Speed = 0.075 mm/s	$\mu = 0.077$ $W = 2.34 \times 10^{-6}$ $\text{mm}^3/\text{N m}$	[105]

For example, composite materials combining carbon nanorod (CNR) fillers with PVDF matrix have been developed to achieve high-tribological performance [103]. The integration of CNR fillers into PVDF enhances the fraction of the nonpolar  $\alpha$ -phase, leading to improved friction and interfacial adhesion properties. The optimal tribological performance was observed with a CNR content of 10 wt.%, where the coefficient of friction dropped significantly from 0.43 to 0.03 and the wear rate decreased from  $8.43 \times 10^{-5}$  to  $3.70 \times 10^{-5}$   $\text{mm}^3/\text{Nm}$ . This indicates that even small amounts of CNR significantly enhance wear resistance of the composite material. In another comparative analysis, friction coefficients of PVDF coatings were evaluated against hot-pressed coatings containing 10 wt.% and 40 wt.% graphene nanoplatelets (GnPs) [101]. The average friction coefficient for PVDF was approximately 0.16, while the coatings with 10 wt.% and 40 wt.% GnPs exhibited lower friction coefficients of about 0.14 and 0.1, respectively, indicating that higher GnPs content leads to reduced friction.

Moreover, friction tests were conducted on PVDF/MoS<sub>2</sub> nanocomposite films in flat-on-flat geometry with varying MoS<sub>2</sub> nanotube concentrations: 0%, 1 wt.%, and 2 wt.% [99]. The addition of MoS<sub>2</sub> nanotubes (NTs) was found to decrease the coefficient of friction. After a 40 m sliding distance, the coefficient of friction for pristine PVDF stood at 0.42, compared to 0.31 for PVDF/1 wt.% MoS<sub>2</sub> and 0.11 for PVDF/2 wt.% MoS<sub>2</sub>. Furthermore, while pure PVDF typically exhibits a phase transition from a nonpolar  $\alpha$ -phase to polar  $\beta$  or  $\gamma$ -phases during friction testing in a boundary lubrication regime, the inclusion of MoS<sub>2</sub> NTs in the composite suppresses the  $\alpha$ -phase, effectively eliminating the visibility of this phase transition.

In addition to improving tribological performance, PFAS composites can also be used to mitigate corrosion-based wear. A novel superhydrophobic composite using PVDF, FEP, and carbon nanofibers (CNFs) was developed exhibiting water-repellent properties [106]. The water contact angle (WCA) was measured at  $164 \pm 1.5^\circ$ , and the slide angle (SA) was recorded at  $5 \pm 0.2^\circ$ . Superhydrophobic surfaces, characterized by a WCA higher than  $150^\circ$  and SA lower than  $10^\circ$ , are highly sought after for their self-cleaning, drag reduction, anti-icing, and corrosion-resistant qualities. Durability tests showed that after 10,000 rubbing cycles, the WCA slightly decreased to  $141 \pm 1.2^\circ$ , and the SA increased to  $20 \pm 0.5^\circ$ , indicating a minor reduction in hydrophobicity due to wear. The coating's

stability under varying pH conditions was also assessed after 15 days of immersion in acidic (pH = 1) and alkaline (pH = 14) solutions; the WCA reduced to  $151 \pm 1.3^\circ$  and  $137 \pm 1.2^\circ$ , respectively. The coating's enhanced corrosion resistance is attributed to its superhydrophobic surface acting as a barrier, increasing the diffusion pathway's tortuosity for gaseous oxygen. PFAS materials can also be reclaimed and recycled into composites, the mechanisms and performance of which are discussed in Section 4.6.

### 2.6. PFAS as Additives

Utilizing PFAS in lubricant additives, exemplified by nano- and microsized PTFE and PVDF particles, helps enhance their friction and wear performance, representing a key advancement in lubrication technology. Such innovations are crucial in developing more efficient lubricants for various applications, including high-stress environments in machinery. Furthermore, the use of extreme pressure (EP) additives in lubricants plays a vital role in protecting metal surfaces against excessive wear under intense conditions. This combination of advanced PFAS additives and EP technology represents a forward stride in lubrication science, offering enhanced performance and greater protection in a wide range of industrial applications where traditional lubricants were found to be insufficient. Table 4 summarizes the different types of PFAS additives along with their tribological performance.

**Table 4.** Various PFAS additives in commercial oils and greases.

Medium	Additive Type	Size and Concentration	Test Parameters	Performance	Refs.
White Oil	PVDF Nanospheres	100 nm 0.1 wt.%	AISI52100 Steel Ball ( $\varnothing = 9.5$ mm) AISI 52100 Steel Disks Load = 5 N Frequency = 2.5 Hz	$\mu = 0.12$ $w = 1 \times 10^{-6}$ $\text{mm}^3/\text{N m}$	[61]
	KH570 modified PVDF Nanospheres	100 nm 0.1 wt.%		$\mu = 0.11$ $w = 0.25 \times 10^{-6}$ $\text{mm}^3/\text{N m}$	
	PTFE filled with Cu	1.5–5 $\mu\text{m}$ 0.3 wt.%	GCr15 Steel ( $\varnothing = 12.7$ mm) Load = 392 N Speed = 1450 rpm/min	$\mu = 0.07$ WSD = 0.55 mm	[107]
	PTFE filled with SiO <sub>2</sub>	1.5–5 $\mu\text{m}$ 0.5 wt.%		$\mu = 0.05$ WSD = 0.55 mm	
150 N Group II Base Oil	PTFE Nano	30–50 nm 8 wt.%	AISI 52100 Steel Ball ( $\varnothing = 10$ mm) AISI 52100 Steel Block Load = 100 N Speed = 50 mm/s	$\mu = 0.11$ WSD = 0.77 mm	[108]
Paraffin Oil	0.25 wt.% RGO + 0.25 wt.% PVDF	180 nm	AISI 52100 Steel Ball ( $\varnothing = 9.5$ mm) AISI 52100 Steel Block Load = 5 N Speed = 24 mm/s	$\mu = 0.13$ $w = 27 \times$ $10^{-8} \text{mm}^3/\text{N m}$	[109]
	0.5 wt.% RGO/PVDF Composite	500 nm		$\mu = 0.10$ $w = 0.48 \times$ $10^{-8} \text{mm}^3/\text{N m}$	
PFPE Oil	None	N/A		$\mu = 0.13$ WSD = None	
	BN Nano	80 nm 0.2 wt.%	Steel Ball Diamond-like Carbon Films Load = 10 N Speed = 50 mm/s	$\mu = 0.07$ WSD = 423 $\mu\text{m}$	[110]
	WS <sub>2</sub> Nano	50 nm 0.2 wt.%		$\mu = 0.03$ WSD = 405 $\mu\text{m}$	
	MoS <sub>2</sub> Nano	50 nm 0.2 wt.%		$\mu = 0.02$ WSD = 472 $\mu\text{m}$	

Table 4. Cont.

Medium	Additive Type	Size and Concentration	Test Parameters	Performance	Refs.
MAC Grease	PTFE Thickener	4 $\mu\text{m}$ 25 wt.%	AISI 52100 Steel Ball ( $\varnothing = 10 \text{ mm}$ ) AISI 52100 Steel Disks Load = 1400 N (max.) Frequency = 25 Hz	$\mu = 0.12$ at $T = 25 \text{ }^\circ\text{C}$  $\mu = 0.14$ at $T = 150 \text{ }^\circ\text{C}$	[111]
PFPE Grease	PTFE Thickener	-	2Cr13 Stainless Steel Ball ( $\varnothing = 9 \text{ mm}$ ) 2Cr13 Stainless Steel Disk Load = 30 N Speed = 400 mm/s	$\mu = 0.2$ at $2 \times 10^{-3} \text{ Pa}$ vacuum	[112]
Lithium Complex Grease	Recycled PTFE Micro	4 $\mu\text{m}$ 25 wt.%	AISI 52100 Steel Ball ( $\varnothing = 12.7 \text{ mm}$ ) Load = 392 N Speed = 1200 rpm	$\mu = 0.07$ WSD = 571 $\mu\text{m}$	[113]

### 2.6.1. Particulate Additives

Incorporating PFAS as additives in lubricants, especially using nano- and micro-sized PTFE particles, has been shown to greatly enhance friction and wear performance. A study blending PTFE particles into a 150 N API Group II base oil at different sizes and concentrations revealed significant improvements in tribological performance [108]. The particles used varied in size from nanoscale (30–50 nm) to micron scale (12  $\mu\text{m}$ ), with two submicron sizes categorized between a smaller range (100–150 nm) and a larger range (300–400 nm), all at an 8% concentration. The study demonstrated the suspension stability of PTFE particles in the oil, as no solid precipitate was observed after seven days. The testing and characterization results revealed that smaller (nanosized) PTFE particles significantly enhance weld load, anti-wear, and friction reduction properties compared to their larger counterparts. Nanosized particles were also found to offer the lowest COF value (0.09) across various particle sizes. Similarly, nanosized particles consistently showed a lower wear scar diameter (WSD), mirroring their reduced friction coefficients. This improvement in both the COF and WSD observed with nanosized particles was primarily due to their enhanced ability to form a protective film on the surfaces of a tribo-couple; a depiction of this is shown in Figure 6.

Using a silane coupling agent (KH-570) can help improve the dispersion of PVDF nanospheres in white oil while averting aggregation [61]. Tribological tests revealed that the friction coefficients of the modified PVDF nanospheres continuously increased under loads lower than 15 N, with a minimum coefficient of around 0.11 at 15 N. However, under loads of 20 N and 25 N, there was a sharp increase in the friction coefficients, peaking at 0.16 and 0.17, respectively. The modification of PVDF particles with KH-570 resulted in the formation of a compact solid film on the substrate, unlike the incompact layer formed by unmodified nanospheres, leading to friction under boundary conditions. Consequently, the COF of KH-570-modified PVDF nanoparticles was higher compared to unmodified ones. Wear rate analysis also showed that both groups with nanospheres had lower wear rates than pure white oil, with the modified group exhibiting enhanced wear resistance due to the stronger nanoparticle–substrate bond formed by KH-570. The compact film deposited by the modified nanoparticles provided better wear resistance, whereas the layer from unmodified particles was looser and more prone to wear.

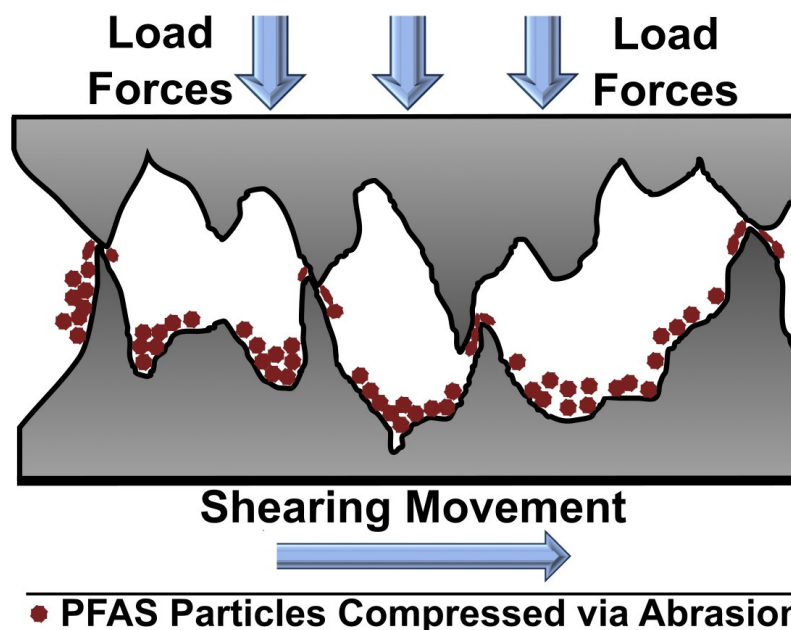


**Figure 6.** Lubrication mechanism of PFAS nanoparticles under shear and contact loading.

#### 2.6.2. Extreme Pressure Additives

Extreme pressure (EP) additives serve a crucial role in lubricants, safeguarding metal surfaces in gears, bearings, and other components from wear under intense conditions. These additives, mixed with engine oils, gear oils, and greases, form a protective film on metal surfaces, inhibiting boundary lubrication regimes and reducing friction during high-pressure interactions. This protective action is essential in preventing severe wear and potential machinery failures.

In lubrication, the concepts from boundary lubrication to fluid film represent critical mechanisms for reducing friction and wear in mechanical systems [114]. The fluid lubricating film operates under conditions where a substantial layer of lubricant separates the moving metal surfaces, primarily through hydrodynamic lubrication. The fluid film thickness, ranging from nanometers to tens of micrometers, acts as a cushion that prevents direct contact between the metal components, ensuring smooth shear and operation [115]. Contrastingly, the boundary lubrication regime possess a higher potential for wear or surface damage, extending to the elasto-hydrodynamic lubrication where EP additives become crucial. The EP additives chemically interact with the metal surfaces to create a protective film of approximately 1 micrometer or less [115]. Despite its minimal thickness, this boundary film is immensely effective in bearing loads and preventing metal-to-metal contact, thereby significantly reducing wear and friction. This transition from fluid lubrication to boundary lubrication underscores a fundamental aspect of lubrication strategies in modern machinery design. As equipment is increasingly expected to operate under harsh conditions, the role of EP additives in facilitating boundary lubrication has become indispensable. By providing a robust protective layer even when traditional fluid films fail, these additives ensure the longevity and reliability of mechanical systems [116].

Recent advancements in EP additives involve integrating nanosized PTFE particles into lubricants to enhance their physical and tribological properties or act as hardening thickeners in greases, forming an effective protective film even under higher loads [11]. This development represents a significant stride in improving machinery performance and longevity in high-stress environments. The friction characteristics of various base stock oils, as classified by the American Petroleum Institute (API), were evaluated in a study using a high-frequency, reciprocating, ball-on-disc configuration. These oils were mixed with PTFE nanoparticles (NPs) as an EP additive, creating nanolubricants (NLs) with 3% PTFE (230 nm) NPs [116]. Compared to virgin oils, the inclusion of PTFE particles significantly enhanced the performance of the oils, particularly showing a 28% improvement in Group

III base oils. Given the exceptional EP performance of these nano-oils, their anti-wear (AW) and antifriction (AF) properties were also investigated. AW tests conducted at varying loads (147, 392, 588, and 784 N) demonstrated that PTFE film formation mitigates metal-to-metal contact, relying on the trapping and smearing of particles in the contact zone. At lower loads, the submicron-sized particles were less efficiently trapped due to greater clearance between the balls. However, as the load increased, the clearance reduced, allowing for more effective entrapment and smearing of particles, thereby creating increasing amounts of PTFE films. Further analysis showed the formation of a thin film of PTFE coating on the balls under enhanced magnification [116]. Notably, this coating remained consistent even under increasing loads, ensuring a smooth PTFE layer that supported the heavier loading conditions by preventing direct asperity contact between the steel balls, thereby boosting the weld load capacity of the NLs. Another study focused on examining the impact of different concentrations (0–6%) of nano-PTFE in 150 N API Group II oil on their physical and tribological properties, utilizing the SRV friction test for evaluation [11]. It was determined that a 3% concentration of nano-PTFE emerged as the most effective among the various nano-oil formulations tested under three different loads.

Most greases can be approximated as a binary system containing a base oil dispersion medium (75–95 wt.%) and a thickener (5–25 wt.%) along with any performance additives. PTFE can serve as an inorganic solid thickener in greases that require an insoluble additive in an inert base oil such as PFPE. Greases with this formulation are typically employed in contact with strong acids, aggressive solvents, magnetic devices, high pressures, and in vacuum. The chemical nature and structure of the added thickener has a significant influence on the lubrication properties of a grease by affecting its rheological properties such as colloidal, thermal, chemical, and mechanical stability. A study probing the effects of various thickeners on the tribological properties of lubricating greases under high pressure and elevated temperature made a comparison between four different grease formulations [111]. The formulations used a multi-alkylated cyclopentane (MAC) base oil and the various individual grease thickeners at a 75 wt.% to 25 wt.% ratio. The test results showed that the PTFE-thickened grease was less stable under an increasing stepped load that maximized at 1400 N and a temperature of 150 °C, reaching a COF of 0.14 compared to a calcium sulfonate complex grease at a COF of 0.1. However, it was able to outperform the commonly used polyurea and lithium complex grease formulations, both of which failed to last the last duration of the test. The results indicate that a PTFE thickener, which when coupled with other synergistic additives, can make up a crucial part of a viable EP grease formulation. The characterization methods used in the study show that the grease formulation containing the PTFE thickener had a more interlocked structure to form a compact network due to increasing interaction between the thickener molecules and the base oil matrix. The resulting higher hardness and improved colloidal stability are properties that help make PTFE an EP additive in its role as a formulation thickener.

### 2.6.3. Synthetic Lubricant Additives

As technology advanced into the late 20th century, the demands on the usage and applications of machinery reached new heights. The advent of the jet age meant that aircraft could reach supersonic speeds, and lubrication systems of gas turbine engines could now expect to routinely reach 600 °F in an oxidizing environment. Furthermore, mankind's newly founded projects in space exploration have opened new environments for the operation of engineering systems, bringing with it several additional performance requirements for lubricants such as large temperature gradients, radiation, weight and volume limitations, and the absence of replenishment. These developments lead to the use of PFAS as a synthetic lubricant in the form of PFPE. Developed by DuPont, the same company credited with synthesizing and producing Teflon, in conjunction with NASA and the United States Air Force for military and aerospace applications, its use was first reported by William H. Gumprecht in 1965 [117]. The PR-143 fluid/PFPE oil described by Gumprecht was characterized for use in hydraulic and gas turbine oils. Its advantageous

properties such as high environmental stability and temperature tolerance, low vapor pressure, and solution insolubility [118] contributed significantly to their superior lubrication performance in challenging conditions. In 1982, the United States Air Force Wright Aeronautical Laboratory put forward several candidates for the expansion of the use of various classes of fluoropolymer base materials for lubricant and fluid materials during a symposium on fluoropolymers [119]. Since then, the applications of PFPE lubricants have greatly expanded.

The temperature–viscosity characteristics of PFPE using the Walther-ASTM equation showed that PFPE has the lowest slope amongst tested lubricants, indicating its superior thermal performance, reducing the average COF while maintaining a consistent wear volume and, unlike ionic liquids, was not subject to supercooling crystallization [120]. PFPE grease formulations with PTFE thickeners can maintain a low and steady COF of 0.2 in a vacuum of  $2 \times 10^{-3}$  Pa, but its performance significantly degrades on exposure to 110 keV of electron irradiation in vacuum due to the decomposition of an acetal group [112]. PFPE is also susceptible to impurities [121], environmental contaminants [122], and thermocatalytic degradation [123], which can rapidly decay its performance and raise concerns over its storage and handling [124]. These issues can be circumvented by pairing PFPE with compatible additives. A study investigating the effects of nanolubricant additives in PFPE oil was able to achieve an initial COF as low as 0.1 under PFPE grease lubrication—this value was unstable as the test progressed, and a COF of 0.13 under PFPE oil lubrication was demonstrated. Nano-MoS<sub>2</sub> additives in PFPE achieved the lowest COF of 0.12 amongst tested additives due to their high compatibility, diffusion behavior, and nanoscale ball bearing to point-like contact at the interface during sliding [110]. PFPE lubricants have also been used in head-disk interfaces of magnetic devices such as hard disk drives [125,126], and are used to lubricate oxygen and nitrous oxide systems in hospitals where any foreign contact could pose an explosion risk [127].

The effects of PFAS in lubricants go beyond just the defined classification of molecules. Lubricants are known to contain several PFAS precursors which can undergo oxidation to form both long and short-chain PFAS molecules. A study showed that improving the dissolution of perfluoroalkyl oligomers in solvent-neutral lubricating oils can help enhance their wear resistance via a 58% reduction in the wear scar diameter, and improve the Equivalent Fuel Economy Index to 4.33 [128]. However, while these effects are beneficial, the addition of these products can lead to the release of additional PFAS and would make the removal of PFAS from lubricant products far more challenging.

A pilot study published in 2020 analyzed the concentrations and profiles of several PFAS molecules used in automotive lubricant oils, hydraulic fluids, and greases in the United States [59]. From a collection of 18 samples obtained off-the-shelf from 9 different brands available commercially, all were found to contain various classes of perfluoroalkyl acids (PFAAs), most commonly perfluoroalkyl carboxylic acids (PFCAs) and perfluoroalkyl sulfonic acids (PFSAs). The detection of these PFAS molecules, via electrospray negative ionization-tandem mass spectrometry (ESIMS/MS), increased by two orders of magnitude after oxidation of the sample, as depicted in Figure 7. Volatile PFAA precursors, such as fluorotelomer alcohols (FTOHs) present in the lubricant products when oxidized, can convert into various PFCAs with varying carbon chain lengths such as PFPeA (C5), PFHxA (C6), PFHpA (C7), and PFOA (C8) at various molar proportions. The oxidation of these precursors is also known to increase PFAS levels found in soil samples taken near oil refineries where many lubricants begin production [129], thus proving that the remediation of PFAS would need to extend to all levels of a lubricant's life cycle.

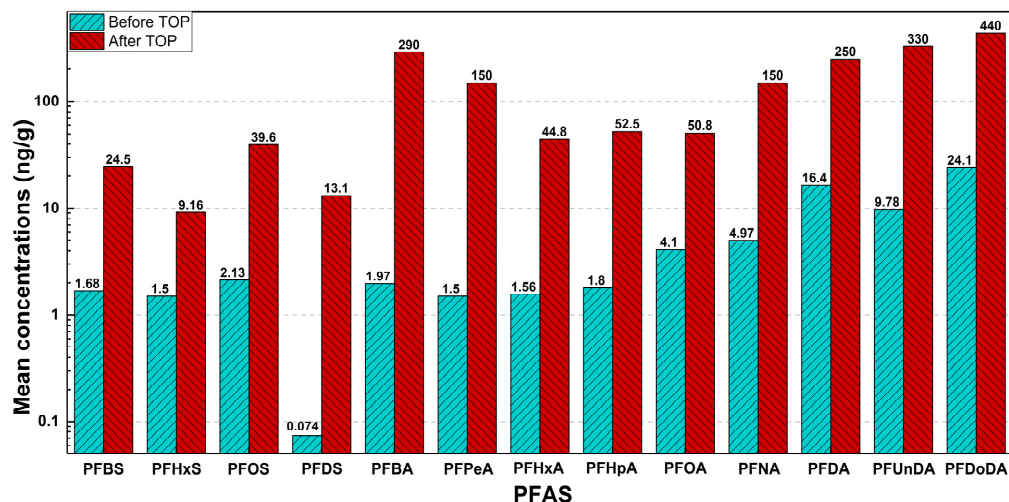


**Figure 7.** Mean concentrations (ng/g) of PFAAs in automotive lubricant oil samples before and after the total oxidizable precursor (TOP) assay processing. Data plotted from [59], Copyright 2020, reproduced with permission from Elsevier.

### 2.7. PFAS in Ionic Liquids

Ionic liquids (ILs), known for their nonflammability, low volatility, and high thermal stability, have emerged as versatile agents in various fields including electrochemistry, synthesis, and lubrication [12,130,131]. Particularly effective as lubricants for extreme conditions, ILs' thermal stability and negligible volatility make them suitable for different alloy tribopairs. The development of biodegradable and multifunctional ILs further enhances their environmental sustainability and utility, offering properties such as anticorrosion and self-healing. In lubrication, ILs' unique structure as liquid salts with organic cations and inorganic anions presents a significant advancement over traditional lubricants. A summary of the frictional performance of ILs is presented in Table 5. Addressing the challenges faced by PTFE, such as severe adhesive and abrasive wear, ILs enhance their self-lubricating efficiency and reliability in moving parts.

**Table 5.** Frictional performance of various Ionic liquids.

Medium	Ionic Liquid	Test Parameters	Performance	Refs.
Liquid	[DMA][OA]	PTFE Ball 304 SS Disc Load = 5 N Frequency = 5 Hz	$\mu = 0.008$	[12]
	[DMA][DA]		$\mu = 0.007$	
Liquid	C <sub>6</sub> F <sub>17</sub> SO <sub>3</sub> P <sub>4444</sub>	AISI5200 Steel Ball (10 mm) Ti-6Al-4V Alloy Disc Load = 5 N Frequency = 25 Hz	$\mu = 0.066$	[13]
	C <sub>8</sub> F <sub>17</sub> SO <sub>3</sub> P <sub>4444</sub>		$\mu = 0.070$	
	C <sub>8</sub> F <sub>17</sub> SO <sub>3</sub> P <sub>8888</sub>		$\mu = 0.073$	
Nanofilm	[Bmim][FAP]	Stainless Steel Sphere (2 mm) Load = 10 mN Speed = 0.20 cm/s	$\mu = 0.150$	[131]
	PFPE Z-tetraol		$\mu = 0.100$	
	EMIM FAP		$\mu = 0.15$	
	HMIM FAP		$\mu = 0.19$	
	BMPL FAP		$\mu = 0.19$	
Additive in Diester Oil	[P <sub>66614</sub> ][NTf <sub>2</sub> ] Concentration: 0.25 wt.%	Disc and Ball: AISI 52100 steel Load = 80 N Frequency = 15 Hz	$\mu = 0.075$	[133]

In a comprehensive study, the lubrication efficiency of Ti-6Al-4V tribopairs using various tetraalkyl phosphonium perfluorosulfonate ionic liquids (TPP ILs) was explored and compared with conventional ionic liquid (IL) lubricants [13]. Six different ILs were analyzed, including three conventional types, 1-butyl-3-methylimidazolium hexafluorophosphate

(L-P104), 1-butyl-3-methylimidazolium tetrafluoroborate (L-B104), and 1-butyl-3-methylimidazolium bis[(trifluoromethyl)sulfonyl]imide (L-F104), along with three perfluorosulfonates ( $C_6F_{13}SO_3P_{4444}$ ,  $C_8F_{17}SO_3P_{4444}$ , and  $C_8F_{17}SO_3P_{8888}$ ). All samples exhibited low friction at low loads. However, as the load increased, the friction also rose, but the increase was significantly lower for the perfluorosulfonate ILs. Notably, the wear volumes for  $C_6F_{13}SO_3P_{4444}$  and  $C_8F_{17}SO_3P_{4444}$  remained almost unchanged, indicating their superior performance as lubricants for Ti alloy tribopairs. This suggests that the TPP ILs, particularly  $C_6F_{13}SO_3P_{4444}$  and  $C_8F_{17}SO_3P_{4444}$ , offer exceptional lubrication properties for these applications.

In another study focusing on AISI 52100 bearing steel/steel pairs, the tribological performance of various ionic liquids, including L-F104,  $C_8F_{17}SO_3N_{4444}$ , and  $C_8F_{17}SO_3P_{4444}$ , was examined and compared to a conventional lubricant (PAO 10) [134]. The results revealed that all the tested ionic liquids maintained low and stable friction coefficients throughout the sliding process, unlike PAO 10. Among the phosphonium-based ionic liquids (PSILs),  $C_8F_{17}SO_3P_{4444}$  stood out by producing a lower friction coefficient than L-F104. The study also found that increasing the fluorocarbon chain length in the IL anion enhanced the wear performance of the ionic liquids under extreme pressure conditions, offering a better outcome compared to L-F104. These findings indicate the potential of specifically formulated ionic liquids, such as  $C_8F_{17}SO_3P_{4444}$ , in improving the lubrication of steel/steel tribopairs, especially under high-pressure environments.

Similarly, two green protic ILs prepared from alkyl amine and long-chain carboxylic acids were applied to PTFE/steel tribopairs, achieving superlubricity in high contact pressure [12]. These ILs outperformed conventional lubricants such as PAO8, PAO10, and PEG400, demonstrating remarkably low coefficients of friction (less than 0.008) and significantly reducing both adhesive and abrasive wear on PTFE. In comparison, PAO10 exhibited the highest COF of 0.035, while PAO8 and PEG400 maintained COFs at 0.023 and 0.016, respectively. The ILs, on the other hand, drastically reduced COFs to the superlubricity range (0.006–0.008), with each IL maintaining an ultra-low and stable value almost without a running-in period. This suggests rapid and effective interfacial interactions facilitated by the ammonium and carboxyl groups. The superior lubrication of these ILs is due to the formation of a thick Stern layer and a tribo-chemical film, as illustrated in Figure 8, a first in achieving superlubricity on soft substrates, guiding lubricant design for PTFE applications. The steel surface's positive charge during friction attracts carboxyl ions, which bind to metallic protuberances electrostatically. Nitrogen groups arrange at the anion layer, developing a shielding Stern bilayer, essential for the lubricating film. The ILs' long alkyl chains enhance the Stern layer's density, aiding in friction pair separation and promoting tribo-chemical reactions. Furthermore, their straight, unbranched chains reduce conformational defects, resulting in a more ordered and effective lubricating film.

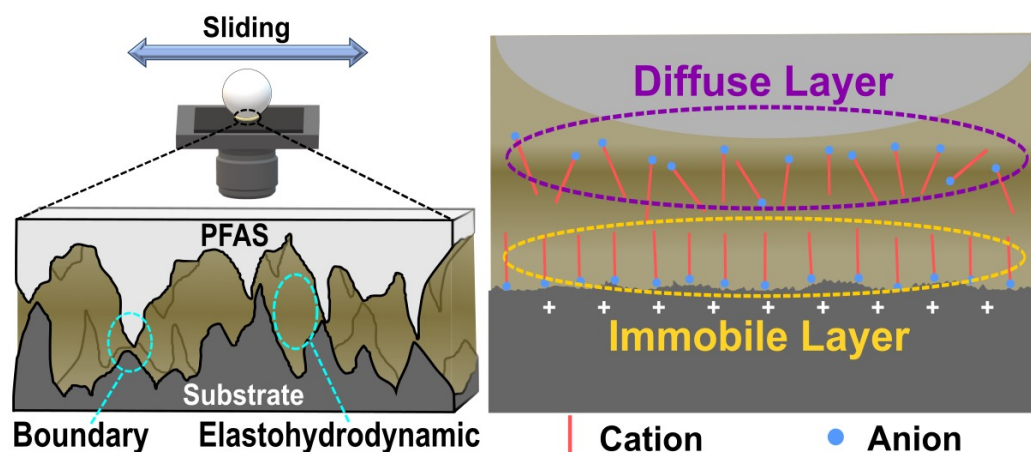


Figure 8. Lubrication mechanism of ionic liquids in a steel/PTFE tribopair.

## 2.8. PFAS in Seals and O-Rings

A secondary source of PFAS pollution in lubrication systems often originates from the use of fluoropolymers in components such as gaskets, seals, and O-rings. Using PFAS in fluoropolymers imbues them with resistance to heat-aging, ozone, chemical and biological attack, abrasion and wear, and low-temperature brittle failure [135]. These properties are ideal for materials that are required to maintain a sealed separation, regardless of environmental conditions and exposure, by retaining their physical properties over their lifetime. However, their ubiquitous use in specialized applications and their designation as polymers-of-low-concern (PLC) make the replacement of these specialty materials particularly challenging [136].

Commonly used fluoropolymers include fluoroelastomer (FKM), fluorocarbon (Viton<sup>®</sup>), fluorosilicone (FVMQ), tetrafluoroethylene propylene (Aflas<sup>®</sup>, TFE/P), and perfluoroelastomer (FFKM). Fluorosilicone is utilized in aerospace for applications such as propellant binders, liquid propellant system bladders, and high-speed aircraft fuel tank sealants [137]. TFE/P, recognized as a high-performance material, is used in various lubrication systems with different engine oils, transmission fluids, and gear lubricants [138], and recently in Lithium-ion batteries as binders for electrode materials [139]. FKM is notable for its widespread usage, owing to its environmental stability, even in extreme conditions, to the high bond energy and chemical structure of the C–F bond. It is typically synthesized through a free radical polymerization process using monomers such as vinylidene fluoride (VDF), *x* hexafluoropropylene (HFP), and hexafluoropropylene (HFP) tetrafluoroethylene (TFE), leading to products such as diaphragms, hoses, wire insulation, and O-rings. However, chemical breakdown or fracturing of C–F bonds in FKM and other fluoropolymers can lead to PFAS leaching into the environment through lubrication or other systems that they are part of. This degradation issue extends to emerging renewable energy technologies such as biodiesels [140] and fuel cell fluids [141], where FKM degradation has been studied.

Observations of aviation lubricant oil, a complex blend of ester or poly-alpha olefin synthetic base oil and antioxidant additives, show evidence of undergoing oxidative reactions at high temperatures and FKM leaching. This is exhibited by the progressive darkening of pure lubricating oil undergoing extensive aging at 200 °C, attributed to the oxidation of antioxidant additives into quinones, which alters the oil's color. The process is further evidenced by changes in the acid value of the lubricating oil post-aging, wherein an increase in acid value over time indicates the formation of acidic substances during the aging process. Additionally, the contact angle between the pure oil medium and fluoroelastomer (FKM) samples decreases as the aging duration increases. As the lubricating oil ages, its small molecule antioxidants eventually get oxidized and lose effectiveness, leading to the oxidation of the base oil's main components. This process can result in the formation of highly polar substances such as carboxylic acids and aldehydes. Consequently, the altered polarity of the aged lubricating oil is reflected by a reduced contact angle and enhanced interaction with FKM. This implies that the aged oil medium exerts a stronger force on the FKM samples and diffuses more readily into them.

Failures of seals and O-rings are typically in the form of compressive stress fractures and thermal cracking due to constituent changes in the FKM structure [142]. A study thoroughly examined the aging behaviors and mechanisms of FKM in lubricating oil (FKM-O) under elevated temperatures [143]. The mechanism behind the breakdown of FKM is a complex process with multiple contributing factors. A study into the FKM aging behavior uses a variety of characterization methods to illustrate the dual mechanisms of dehydrofluorination and polymer crosslinking breakdown, as shown in Figure 9 [143]. Changes in the chemical structure of FKM were detected and characterized by attenuated total reflection-Fourier transform infrared spectroscopy (ATR-FTIR), where spectra band intensity decreases showing the reduction of fluorine content in the rubbers due to the elimination of the hydrogen fluoride through dehydrofluorination. A large number of C=C bonds are broken in the high-temperature oil medium to produce PFAS fragments of different molecular sizes, and the fracture of C–F bonds to generate HF. Another mecha-

nism involves the physical diffusion of the lubricant medium into the rubber acting as a plasticizer, which, coupled with O-ring swelling or the cyclic stresses on seals, can cause the elastic retraction of the network structure. The destruction of crosslinks can lead to the failure of the exposed FKM material and is evidenced by the decrease of mechanical properties such as tensile strength, storage modulus, crosslinking density, and glass transition temperature ( $T_g$ ).

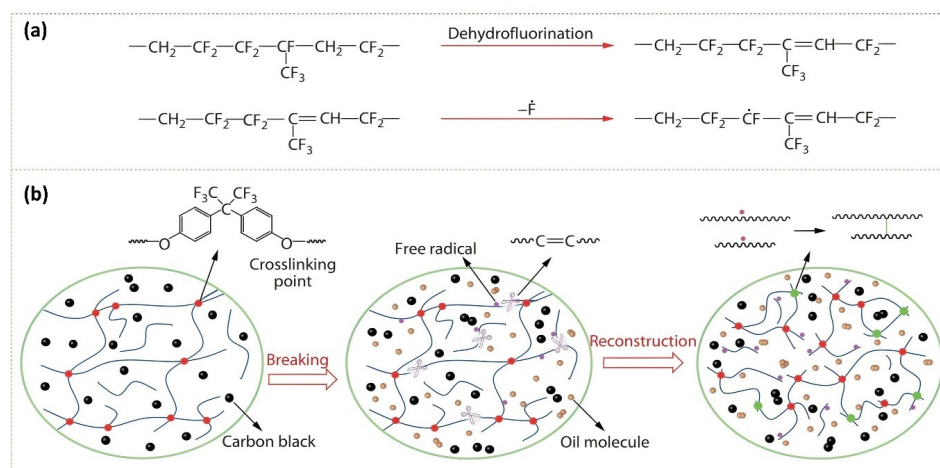


**Figure 9.** (a) Chemical reactions and (b) network structure of FKM degradation in oil [143]. Copyright 2020, reprinted with permission from Springer Nature.

### 3. Impacts of PFAS

Understanding the exposure routes of PFAS is crucial for comprehending the environmental impact and risks posed by these substances. The movement of particles from lubricants to undesired locations constitutes environmental pollution and unwanted exposure. This creates a critical interface between humans and PFAS in the environment, known as the human–environment interface. Direct contact with lubricants containing PFAS represents another exposure pathway, termed the human–lubricant interface. These interactions can result in pollution, environmental damage, and significant health risks due to the toxicological effects of PFAS. Exposure at the human interface is readily observed to occur through three primary mechanisms: inhalation, ingestion, and dermal contact. Inhalation involves PFAS entering the lungs via airborne vapors or particles. Ingestion refers to the intake of PFAS through eating or drinking contaminated substances, including food and water. The third route, dermal contact, occurs when PFAS makes contact with human skin or enters the body or bloodstream through cuts or other openings. These exposure pathways highlight the need for research, awareness, and preventive measures to mitigate the risks associated with PFAS in lubricants.

#### 3.1. Environmental Impacts

PFAS contamination, both to the environment and to humans, can occur from the direct exposure to lubricant products containing PFAS, or from exposure to PFAS due to pollution [144]. Generally, when a lubricant is lost to the environment, the PFAS additives will be lost with it. Typical examples of environmental pollution due to lubricants are caused directly or indirectly by humans. Oil or grease spills can result from the improper handling and/or disposal of the oil, or can occur incidentally. In a closed lubrication system, after the lifetime of the lubricant has been met, and the used lubricant is collected and disposed of, spillage and draining to the environment may occur. Out of all the oil and grease lubricants used, 10% of waste lubricants produced from mechanical systems are discarded directly into the environment [145]. This is seen passively in mechanical joints and surface interfaces of heavy equipment or vehicles that experience frequent motion in open atmosphere conditions. These interfaces utilize grease and oils to function effectively

over their service times where parts of the lubricant and surface material wear out. The worn material and lubricant are then lost from the working system and transferred to the environment.

Lubricant–environment pollution poses a problem for ecosystems, human infrastructure, and human health. Figure 10 demonstrates how PFAS can travel through an ecosystem and infrastructures to become PFAS sources which humans are exposed to due to everyday nutrition needs. PFAS particles typically deposit into the soil through two main modes of transit: air and water [19,146]. Water contamination is a primary concern when observing the interface with the environment and humans. Upon contamination of a water source, bacteria in the water can absorb PFAS substances found in lubricants, which are then consumed by larger organisms [147]. The particles work their way up the food chain into fish or other animals which humans typically consume [147]. By eating animals that have been exposed to PFAS, humans are then likewise exposed to a concentration of PFAS. Humans can also more directly ingest PFAS from water sources containing particulates of PFAS. A study gathering data from 2016 to 2021 took water samples from over 700 public and private drinking wells in the United States. They found that the sum of total PFAS tested for was a median of 7.1 ng/L for public wells and 8.2 ng/L in private wells [148]. Modern in-home filtration systems can help to reduce the amount of PFAS in tap water, but completely negligible removal is not possible with an at-home system [149].

PFAS pollution may readily come from the mechanical applications which utilize it, but it is also spread or leached into the surrounding environment close to manufacturing sites which create products containing PFAS [150]. Analyzing PFAS concentrations in air, a study conducted at a manufacturing site found that the mean daily inhalation of PFOA (commonly used when manufacturing PTFE) in a 20 km area was 2.15 ng/day in adults [150,151]. Focusing on soil pollution, sorption/desorption of PFAS in soil can occur from different mechanisms dependent on the soil characteristics, pH, organic material, and soil composition [82]. The mechanism depends also on water quality, as well as PFAS functional groups and their carbon chain lengths present in the system [82]. PFAS which have adsorbed into soil and water can also be taken up by plants and crops [152]. PFAS exposure happens not only from ingesting animals or substances containing PFAS, but also from the coatings and surfaces of tools and packaging used to prepare food. Humans who utilize PTFE cookware can be exposed to the ingestion of particles by simply boiling water. One study found that an adult can become exposed to about 65 ng of PFOA from drinking 100 mL of water boiled in a PTFE-coated container [59]. Other applications of PTFE, dental floss, food service, or medical devices, make this PFAS coating particularly prominent in the human–lubricant interface [153].

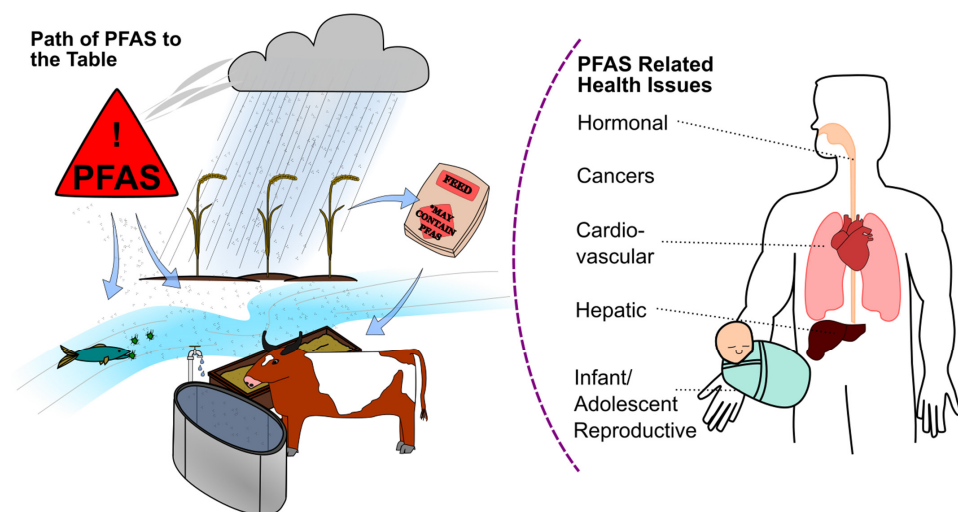


**Figure 10.** Path of PFAS through the environment from the source via air, water, and soil into animals meant for consumption. PFAS concentration in the body can lead to serious health problems.

### 3.2. Human Health and Toxicology Impacts

The persistent nature of PFAS presents both advantages and disadvantages; their capacity to stay in the environment and accumulate in the bodies of humans and animals raises substantial concerns. Extensive research, including studies by DuPont and 3M since the early 1960s, has linked PFAS exposure to systemic and liver toxicity, reproductive issues, and increased risks of cancer, underscoring the complex interplay between their industrial utility and environmental and health impacts [154]. The health consequences of PFAS exposure are similarly worrisome. Studies have established a connection between PFAS and several negative health effects, such as specific forms of cancer, weakened immune system function, harmful effects on reproduction and development, disruption of hormonal balance, and elevated levels of cholesterol. These findings have ignited a worldwide discussion on the safety and control of PFAS, prompting scientists and industry professionals to explore safer substitutes and devise efficient strategies for reducing their influence [155]. The Agency for Toxic Substances and Disease Registry (ATSDR) has publicly available documents regarding the toxicological effects of substances in animals on specific anatomical systems in the body [156]. In animals, a metric that is used to describe the concentration to induce death in 50% of a population is known as an LD50, or a lethal dosage 50 [157]. This is typically not useful when considering substances such as PFAS, due to their frequent, but low concentrations at which they may enter the human body [62]. Metrics that are presented and used in the studies collected in the ATSDR profile on PFAS are lower observed adverse effects level (LOAEL), and (NOAEL) [63]. These are known as threshold dosages [157,158].

The ATSDR PFAS profile highlights the importance of studying the consequences of PFAS, namely its influence on the liver, developmental processes, and reproductive health [158]. Figure 10 highlights some of the notable health concerns associated with PFAS which have been shown in the PFAS profile and other literature. The profile includes PFAS such as perfluorooctane sulfonic acid (PFOS), PFOA, perfluorohexanesulfonic acid (PFHxS), and PFOSA, whose toxicological characteristics inform legislation and safe human exposure levels. Recent global research has provided a clear understanding of the harmful impacts of distinct PFAS, which demonstrates a range of toxic consequences reported in various organisms when exposed to varied conditions [159–168].

Prominent discoveries indicate that POSF has the capacity to induce cancer in people, especially among those who have been exposed to fluorochemical production facilities in the United States [159]. Furthermore, it emphasizes the potential danger of hyperuricemia in those who are exposed to PFOA and PFOS close to a chemical facility, once again within the United States [160]. In Europe, leukemia has been associated with exposure to PTFE in production facilities [161]. Postnatal exposure to PFDA and PFOA in children under 13 has been linked to changes in diphtheria antibody levels [162]. In Britain, PFNA and PFHxS exposure during pregnancy has been linked to alterations in birth size in male infants [163]. PFAS exposure in aquatic habitats, specifically in Korea [164] and Belgium [167], has been associated with reproductive abnormalities in Japanese medaka [164] and the accumulation of PFAS in fish intestines through biomagnification, respectively. In the USA, a biomonitoring program conducted in New Jersey aimed to measure the levels of PFAS in serum, revealing the extensive prevalence of PFAS exposure [168]. Finally, a study conducted on mice revealed that exposure to a diet that promotes the development of atherosclerosis and water contaminated with PFAS resulted in elevated levels of cholesterol, sterol metabolites, and bile acids in their bloodstream [166].

### 4. PFAS Remediation and Alternatives

The management and mitigation of PFAS requires a comprehensive approach: integrating regulatory considerations, advanced degradation methods, recovery techniques, and developing safer alternatives. Understanding the ever-changing regulatory environment and industry practices is essential for shaping effective strategies for handling PFAS. This is complemented by exploring waste remediation methods such as thermal and electrochem-

ical degradation, modified with promising techniques for neutralizing these persistent compounds. Several other techniques such as low/high-temperature thermal desorption, incineration, vapor energy generator, electrical discharge plasma, and microwave hydrothermal treatment have also been employed [26]. Biodegradation methods offer a natural and sustainable solution for PFAS pollution, although they face specific challenges in breaking down these chemicals. In addition to degradation, the recovery and recycling of PFAS can minimize its environmental impact, calling for innovative approaches to repurpose these substances. The pursuit of PFAS alternatives is of paramount importance. Identifying and implementing safer, environmentally friendly substitutes could play a significant role in reducing the reliance on PFAS, and even other industry additives, while mitigating their long-term effects. Together, these components form a holistic approach to addressing the complex issues surrounding PFAS usage and its environmental implications.

#### 4.1. Regulatory Considerations and Industry Practices

Following studies on the hazardous impacts of PFAS on the environment and humans, government and environmental organizations have developed and enforced guidelines, policies, and regulations regarding PFAS and products containing PFAS. The most prominent of these groups in the United States is the Environmental Protection Agency (EPA) [169]. In the European Union, the European Chemicals Agency (ECHA) controls and regulates restrictions on chemicals [170]. International efforts help to guide the restriction of PFAS in countries around the world. Beginning in 2009, the Stockholm Convention on Persistent Organic Pollutants (POPs), a treaty to protect the environment and humans from dangerous chemicals, listed its first restriction on a PFAS, PFOS [171,172]. If a substance is listed as a POP, then by the treaty, signing countries are bound to eliminate or restrict the substance, depending on the chemical [171]. Presently, PFAS listed as POPs include the ever-popular PFOS, PFOA, and PFHxS [172].

In the United States, the EPA is currently executing a roadmap from 2021 to 2024 which outlined specific courses of action regarding PFAS [173]. This roadmap sets goals to conduct research in all the areas addressed in this review, restrict PFAS in industrial applications, and remediate to bring corrections and settlements to people who are exposed and impacted by PFAS [173]. The European Commission launched the Green Deal in late 2019 with an overarching goal of climate neutrality by 2050 [174]. The Green Deal pushes broader environmental policies and legal alignment with the views of the EU than the EPA PFAS Roadmap outlines, but both initiatives mandate restrictions and monitoring of PFAS in water [173,175]. There is also a push to further classify PFAS under several “essential use” categories to informatively regulate PFAS usage and better manage the accelerated transition to alternatives. The methodology is based on an older approach prescribed in the Montreal Protocol that was immensely successful in phasing out ozone-depleting chlorofluorocarbons (CFCs) [176,177].

#### 4.2. Electrochemical Degradation Methods

##### 4.2.1. Electro-Oxidation

Electro-oxidation (EO) is a novel technique that produces different reactive species using reactions involving oxidation at the anode and reduction reactions towards the cathode [178]. It can help degrade organic chemicals that cannot be broken down naturally, and can also remove some inorganic species [179,180]. The effectiveness of EO depends on operational factors such as the choice of electrode materials, concentration of electrolyte, current density, pH level, etc. [179,181,182]. Electro-oxidation can be carried out through two distinct processes: direct electro-oxidation and indirect electro-oxidation, as illustrated in Figure 11a. Direct electro-oxidation, also referred to as anodic oxidation, is a straightforward and highly effective advanced oxidation process (AOP) used to degrade pollutants. This approach produces potent oxidizing agents, mainly hydroxyl radicals, through either direct electron transfer to the anode or surface reactions [183,184]. The process occurs in two distinct stages: initially, the pollutant disperses and moves from the main solution

towards the surface of the anode, and then undergoes oxidation at the anode surface [185]. Unlike direct electro-oxidation, indirect electro-oxidation employs electrochemical reactions to generate powerful oxidizing agents such as chlorine, ozone, and hydrogen peroxide directly in the solution near the electrodes [185]. Amongst these, chlorine is the predominant oxidizing agent, generated through the process of anodic oxidation of chloride [186].

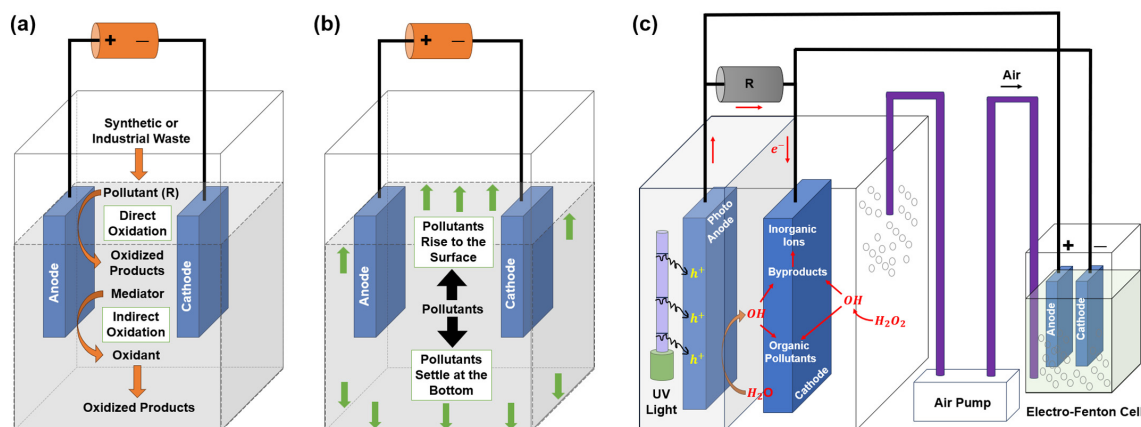


**Figure 11.** PFAS purification techniques: (a) electro-oxidation and (b) electro-coagulation [185], Copyright 2023, redrawn with permission from Elsevier. (c) Illustration depicting the operational process of a standard photocatalytic fuel cell [187], Copyright 2020, redrawn with permission from Elsevier.

#### 4.2.2. Electro-Coagulation

Electro-coagulation (EC) is an emerging electrochemical technology that is increasingly being recognized as an environmentally friendly substitute for conventional chemical coagulation in water treatment. This technique uses electrical energy to produce coagulant substances in water, reducing the requirement for external chemicals. The core of EC is the interaction between electricity and metal electrodes, commonly iron (Fe) or aluminum (Al) plates, as shown in Figure 11b [185]. Applying a direct voltage causes the anode, which is positively charged, to undergo electro-dissolution, resulting in the release of metal ions into the water [188–190]. These metal ions undergo chemical interactions with water and other dissolved components, transforming into several coagulant species such as hydroxides and oxyhydroxides. The newly formed coagulants act as magnets, attracting and agglomerating suspended particles, contaminants, and pollutants in the water. This creates larger, heavier flocs that readily settle out of the water or can be easily removed by filtration.

#### 4.2.3. Photocatalytic Fuel Cell

The utilization of solar energy to propel reactions in photocatalytic fuel cells (PFCs) underscores their capacity as a sustainable and energy-efficient approach for decomposing PFAS in contaminated water. The ultimate objective of this procedure is the total conversion of PFAS into innocuous end products such as carbon dioxide, water, and inorganic fluoride by mineralization. PFCs embody an innovative methodology that combines photocatalysis and electrochemical processes, as depicted in Figure 11c. During this method, a semiconductor photocatalyst, such as  $\text{TiO}_2$  or  $\text{V}_2\text{O}_5$ , is stimulated by ultraviolet (UV) light to produce electron-hole pairs that possess substantial oxidative and reductive potential [187,191]. These pairs generate reactive oxygen species (ROS), such as hydroxyl and superoxide radicals, which are capable of efficiently breaking the robust C–F bonds in PFAS. This results in the decomposition of PFAS into smaller, less detrimental compounds. Concurrently, electrochemical activities taking place at the PFC's electrodes—oxidation at the anode and reduction at the cathode—also promote the degradation of PFAS. The efficiency of photocatalytic degradation in PFAS removal is contingent upon various parameters, including the nature of the specific PFAS compound, the employed degradation techniques, the duration of the reaction, and the participation of oxidative or reductive

species, etc. [192]. Furthermore, the introduction of specific metal ions into the photocatalyst lattice can demonstrably enhance the degradation efficacy [192]. Ongoing research efforts are dedicated to improving the effectiveness of PFCs and comprehending the byproducts generated during their breakdown, thus strengthening their potential as a viable remedy for PFAS pollution.

#### 4.3. Thermal Degradation Methods

##### 4.3.1. Sonochemical Degradation of PFAS

Sonochemistry harnesses the power of acoustic fields to instigate the formation of radical species, thereby facilitating the degradation of contaminants across various aqueous environments [193]. This process, known as sonolysis, leverages ultrasonic irradiation to generate pressure waves that induce the formation of minute cavities within the liquid medium [194,195]. The interaction of sonowaves with an aqueous solution result in localized regions of alternating low and high pressure, fostering the creation and subsequent collapse of vapor bubbles (a phenomenon termed cavitation) under extreme temperature and pressure conditions [196]. These fleeting moments of elevated temperature contribute to the in situ thermal decomposition of water within the interfacial and vapor regions of each collapsing bubble, yielding hydrogen atoms (H), oxygen atoms (O), and highly reactive hydroxyl radicals ( $\bullet\text{OH}$ ) [197]. These liberated radicals engage in rapid reactions with contaminant molecules either at the bubble interface or within the gas phase contained within the bubble itself [198].

##### 4.3.2. Subcritical or Supercritical Treatment of PFAS

An environmentally friendly approach to water treatment utilizes water's supercritical and subcritical conditions for PFAS contaminant destruction [194]. For water, the supercritical conditions correspond to a pressure higher than 22.1 MPa and temperature higher than 374 °C. Subcritical conditions occur when the water temperature is maintained between 100 °C and 350 °C under pressurized conditions such that the water exists in the liquid phase. Several studies have been conducted to investigate PFAS degradation behavior under subcritical and supercritical conditions [199–202]. The results indicated that PFOS exhibits minimal degradation inside pure subcritical water, but the degradation rate dramatically increases when metal powder is added in the subcritical water [199,200]. Similar trends were observed at supercritical conditions where ZVI addition in pure supercritical water accelerated the degradation reaction [201,202].

#### 4.4. Biodegradation Methods

##### 4.4.1. Microbial Degradation of PFAS

A majority of PFAS substances exhibit a neutral character and demonstrate resistance to biodegradation mechanisms, both factors contributing to their environmental persistence and challenges in their natural degradation. Within the perfluorocarboxylic acids (PFCAs) class of PFAS substances, perfluorooctanoic acid (PFOA) has been extensively studied for its resistance to microbial transformation and defluorination. The microorganism *Pseudomonas parafulva* YAB1, found in soil, was observed to convert approximately 48% of PFOA into other products [203], while *Acidimicrobium* sp. A6 demonstrated its ability to defluorinate PFOA by breaking down over 60% of PFOA and PFOS in 100 days, but would result in fluoride release as wastewater treatment plant sludge [204] and ferrihydrite-enriched biosolids [205]. A study employing a microbial electrolysis cell (MEC) instead of Fe(III) [206] as an electron acceptor demonstrated a 77% reduction in PFOA levels, along with fluoride release and the formation of four altered compounds (PFBA, PFHxA, PFHpA, and PFPeA), indicating a potential breakthrough in microbial defluorination strategies.

Perfluorooctanesulfonic acid (PFOS), another class of PFAS, showed extreme resistance to microbial degradation despite performing substantial anaerobic transformation studies spanning 259 days [207]. Four electron suppliers (acetate, ethanol, hydrogen gas, lactate), five different microbial communities, and several electron acceptors were used, but no

indications of biotransformation or defluorination were observed. Progress was made when Kwon et al. [208] reported a 67% decrease in PFOS after a 48 h aerobic incubation with using *Pseudomonas aeruginosa* HJ4 from wastewater treatment plant (WWTP) sludge. The most thorough study on microbial PFOS degradation involved strain A6, which facilitated the removal of up to 60% of PFOS over 100 days, starting from an initial concentration of 100 µg/L [204].

The breakdown of fluorotelomer alcohols (FTOHs) is frequently quoted as the origin of PFOA and other PFCAs in the environment, making this class of compounds the focus of considerable attention. FTOHs, unlike other PFAS, have a quick microbial breakdown (within a few days to weeks) under aerobic conditions, producing aldehydes and PFCAs. Substantial investigations have been carried out to examine the conversion of 6:2 FTOH and 8:2 FTOH in various environmental conditions, such as activated sludge, soil, sediments, and specified microbial communities. The conversion products found regularly consist of fluorotelomer aldehyde (FTAL), perfluorooctanoic acid (PFOA), fluorotelomer carboxylic acid (FTCA), and short-chain PFCAs [209–212]. Under aerobic conditions, FTOHs are initially oxidized to FTAL, which then undergoes further transformation to FTCA. Finally, FTCA is decreased to FTUCA, resulting in the discharge of a fluoride ion. The process of anaerobic biotransformation using 8:2 FTOH [213] results in the formation of 7:2 olefin, 7:2 sFTOH, and nonthreatening products such as PFHpA, PFHxA, PFBA, and PFOA [21,214,215].

#### 4.4.2. Enzymatic Degradation of PFAS

Enzymes are helpful catalysts in the biodegradation of PFAS, yet identifying the specific enzymes and their defluorination mechanisms remains largely unexplored. Although the biodegradation of various PFAS has been documented, there's a notable research gap in the biodegradation and defluorination of prevalent C8 perfluoroalkyl compounds such as PFOS and PFOA [204,205]. A significant challenge, as highlighted in studies [216,217], is the characterization and detection of enzymes responsible for these processes, particularly those that break down branched PFCA.

Research has mostly concentrated on simpler organofluoride compounds, including fluoroacetates, perfluoroethers, and fluorinated aromatics. Fluoroacetate dehalogenases (FAcDs) are notable enzymes that break the C-F bond in fluoroacetates. These enzymes are sourced from various bacteria such as *P. fluorescens*, *Pseudomonas* sp. strain A, *Burkholderia* sp. FA1, *Deftia acidovorans*, *Synergistetes* strain MFA1, and *Moraxella* [218–222], and are benchmarks in enzymatic defluorination studies. They have been extensively researched to understand the defluorination process, given the C-F bond's toughness, the rarity of PFAS biodegradation in nature, and fluoroacetate's toxicity. Studies employing crystal structures, mutagenesis, and molecular dynamics/molecular mechanics [223] have provided insights into the defluorination mechanism, particularly highlighting the Asp-His-Asp triad's role in catalysis. Another category of recognized dehalogenases for fluorinated compounds includes 4-fluorobenzoate dehalogenases, transforming 4-fluorobenzoate into fluoride ion and 4-hydroxybenzoate [222]. Understanding the degradation mechanisms that drive these enzymes is critical, though the complexity of their interactions presents ongoing challenges in this field.

#### 4.5. PFAS Alternatives

In the wake of regulations asserting the phasing out of PFAS, the need for new substitutes has emerged, incorporating structural modifications to match performance and ease degradation. These alternative PFAS varieties feature shorter fluoroalkyl chains and structures with ether linkages or chlorinated carbons instead of exclusively fluorinated carbons [224]. The utilization of short-chain PFAS as alternatives to their long-chain counterparts has been extensively employed [225]. Short-chain PFAS exhibit greater water solubility and hydrophilicity compared to their long-chain counterparts, rendering them more efficacious in certain contexts, such as the formulation of firefighting foams [34,226]. In addition, it is worth noting that short-chain PFAS exhibit a reduced propensity for

bioaccumulation and demonstrate lower levels of acute toxicity when compared to their long-chain counterparts. Consequently, there is a reduced likelihood of bioaccumulation occurring in the organisms of both animals and humans as a result [225,226]. The United States Environmental Protection Agency (EPA) has established a definition for “short-chain PFAS” as perfluorocarboxylic acids (PFCAs) with a carbon chain length of fewer than eight, and perfluorosulfonic acids (PFSAs) with a carbon chain length of less than six [34].

In the quest for environmentally sustainable and health-safe alternatives to PFAS, several promising candidates have emerged, as demonstrated in Table 6. Silanes and polyphosphazenes, known for their specific functionalities, offer varying degrees of water and oil repellency, though they may not always reach the high-performance levels of PFAS in aspects such as low friction coefficients or chemical resistance [227,228]. Telomer-based fluoropolymers, characterized by shorter chains with alternating carbon and fluorine atoms, along with oligomeric siloxanes (OBS) featuring silicon-oxygen (Si-O) bonds and organic side groups, present a structural difference that potentially makes them less persistent and more biodegradable than traditional PFAS [119,229,230]. Hexafluoropropylene oxide trifluoroacetate (HFPO-TA) and hydrofluoroethers (HEPs) also stand out as viable substitutes. HFPO-TA, with shorter chains and an ether linkage, is theorized to be less persistent in the environment [231,232]. Novel nonfluorinated polymers (NNNs) and polyhydroxyalkanoates (PHAs) are being developed with an emphasis on environmental friendliness. NNNs, designed to be biodegradable or with shorter chains, along with PHAs, which are biodegradable under natural conditions and can be produced from renewable resources, provide sustainable and nontoxic alternatives to PFAS [233,234].

**Table 6.** Potential PFAS alternatives in tribology.

PFAS Alternative	Chemical Formula	Applications	Refs.
Silanes	$\text{Si}_n\text{H}_{2n+2}$	Coatings, adhesives, lubricants, electronics	[227,235]
Polyphosphazenes	$[\text{NP}(\text{R}_1)(\text{R}_2)]_n$	Fire-resistant materials, membranes, adhesives	[228,236]
Telomer-based fluoropolymers (C6O4)	$\text{C}_6\text{F}_{12}\text{O}_4$	Coatings, membranes, lubricants, fire retardants	[229,237]
Oligomeric siloxanes (OBS)	$(\text{R}_2\text{SiO})_n$	Coatings, adhesives, cosmetics, electronics	[230,238]
Hexafluoropropylene oxide trifluoroacetate (HFPO-TA)	$\text{C}_3\text{F}_6\text{O}_3$	Solvents, cleaning agents, electronics	[231,239]
Hydrofluoroethers (HEPs)	$\text{C}_2\text{F}_6\text{O}$	Solvents, cleaning agents, electronics	[232,240]
Novel nonfluorinated polymers (NNN)	Variable	Coatings, lubricants, textiles, membranes	[233,241]
Polyhydroxyalkanoates (PHAs)	$[-\text{O}(\text{CH}_2)_m\text{CHOH}-]_n$	Biodegradable plastics, coatings, adhesives	[234,242]

#### 4.6. PFAS Recovery and Recycling

While avoiding the release of PFAS by using proposed alternatives is a guaranteed way to meet upcoming regulations, the question of what to do with existing PFAS waste still remains. Currently, about 83.5% of fluoropolymers are subject to incineration—an expensive and pollution-emissive process, but deemed necessary to help breakdown long-chain PFAS polymers and materials such as PTFE. Recycling accounts for only 3.4% of fluoropolymer disposal with the rest ending up in landfills [136]. There is also a case to recover the manufacturing expenses associated with PFAS, particularly compounds such as fluorosurfactants, which are up to 1000 times more expensive than traditional hydrocarbon surfactants [243].

In the context of environmental sustainability and resource conservation, the innovative recycling of polymers, particularly those in the PFAS family, is a pioneering venture in the field of advanced materials research [244,245]. This exploration focuses on transforming discarded polymer materials into high-quality tribological composites without emissions, a significant stride towards sustainable engineering. By employing advanced recycling techniques, these polymers are repurposed into micropowders, which are then integrated with specialized additives to enhance their performance in lubrication applications [245]. The resulting composites exhibit tribological properties that are akin to those made from virgin materials, showcasing the feasibility and efficiency of this recycling approach. The successful application of these recycled polymers in lubrication systems not only contributes to reducing environmental impact, but also opens new avenues for cost-effective and eco-friendly material innovations [105,113]. These recycling methods serve as a testament to the principles of circular economy and the philosophy of cradle-to-cradle in the materials industry, reimagining waste not as an endpoint, but as the genesis for crafting cutting-edge, eco-conscious materials.

An example of this technique being used in a lubricating substance explored the creation of high-performance lithium complex grease, integrating low molecular weight recycled PTFE microparticles as an extreme pressure (EP) additive [113]. These microparticles are derived from presintered PTFE scrap through a meticulous process of E-beam scissoring and ultra-high-speed grinding, as shown in Figure 12. Primary recycling involves processing preconsumer polymers through extrusion or other mechanical techniques for pure polymer streams [245]. The transformation of high molecular weight PTFE into micropowders is achieved through either thermo-mechanical degradation or high-energy radiation degradation. Common radiation sources used in this process, often found in medical technology, include Gamma-radiation from a  $^{60}\text{Co}$ -source and Beta-radiation, specifically E-Beam. Following irradiation, a grinding step is integral to attain the required particle size, and is particularly useful in extreme pressure applications in grease formulations.

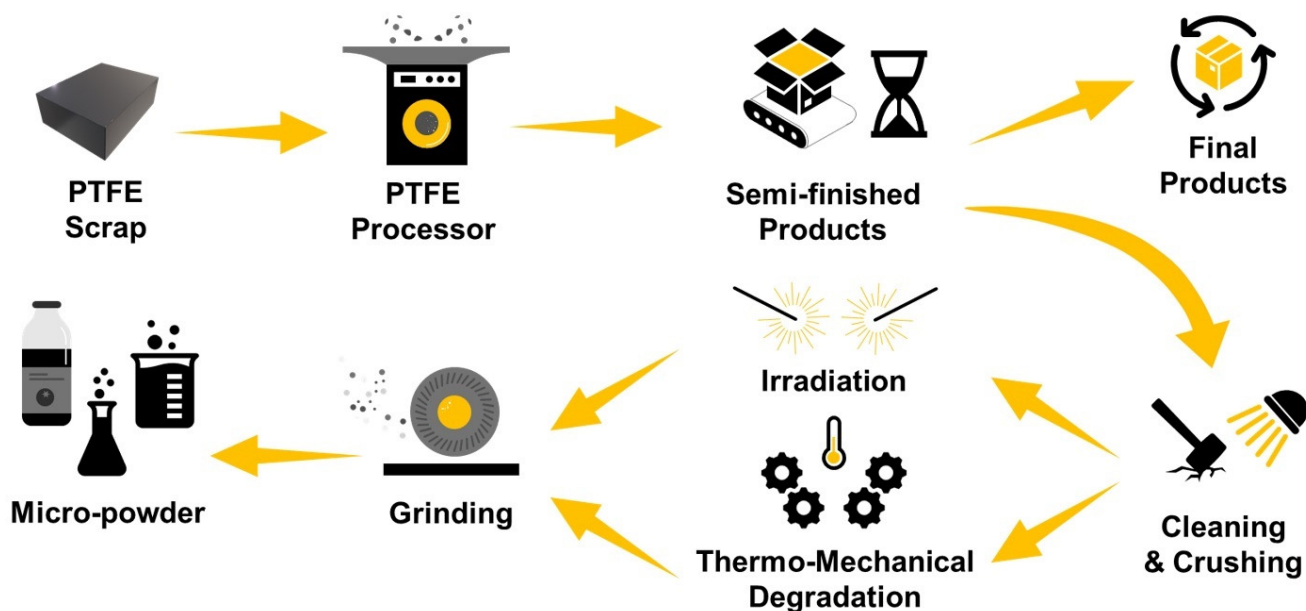


**Figure 12.** Recovery circuit for PTFE [246]. Reproduced with permission from recycling of fluoropolymers, pro-K fluoropolymergroup.

These recycled PTFE micropowders were employed as additives into Lithium-based grease and compared with  $\text{MoS}_2$  additives [113]. Frictional behavior analysis over a one-hour test highlights a notable decrease in the coefficient of friction (COF) for grease samples containing PTFE, attributed to its better sliding characteristics compared to Molybdenum (Moly). Wear scar diameter (WSD) measurements further reveal that PTFE grease induces

only slight changes in WSD values, demonstrating less wear compared to the Moly-grease. Furthermore, PTFE grease achieved friction coefficient reductions of 14.4% (ramp up) and 33.8% (ramp down), and a decrease in WSD by 36.8% and 34.1%, respectively, when benchmarked against the Moly-grease. These findings underscore the enhanced wear and friction protection offered by PTFE microparticles compared to moly grease under the tested conditions.

A novel upcycling approach utilizes waste PVDF membranes, converting them into a self-lubricating composite material, as shown in Figure 13. Initially, the PVDF membranes undergo extensive cleaning via ultrasonic treatment in various solutions, ensuring the removal of strains and impurities. A solvent recovery method using DMAc solvent was employed to dissolve the treated PVDF membranes, followed by a phase inversion technique to precipitate and purify the PVDF, resulting in high-purity PVDF solid powders. These powders were further processed into micropowders using a solution precipitation method involving the dissolution of PVDF and PVA in DMAc, the addition of a precipitant solution, and subsequent stirring, centrifugation, and drying. The process achieved an approximate yield of 83.5%. The recycled PVDF micropowders served as the polymer matrix in the composite, while microcapsules consisting of polysulfone (PSF) encapsulating lubricant oil (PAO) were incorporated as fillers. The investigation highlights that composites fabricated from recycled PVDF membranes exhibit tribological characteristics comparable to those made from virgin PVDF micropowders. The performance of the PAO@PSF/PVDF composite with 20 wt.% PAO@PSF microcapsules stand out, demonstrating optimal performance with a friction coefficient of 0.077 and a wear rate of  $2.34 \times 10^{-15} \text{ m}^3/\text{Nm}$ . Comparative analysis of neat PVDF and PVDF composites with microcapsule additions, sourced from both recycled and virgin PVDF, revealed similar tribological properties. For composites with a 20 wt.% microcapsule concentration, friction coefficients and wear rates were nearly identical between recycled and virgin PVDF sources, underscoring the minimal distinction between them. This innovative recycling and repurposing of PVDF membranes not only demonstrates a practical approach to waste management, but also contributes to the development of advanced tribological materials.

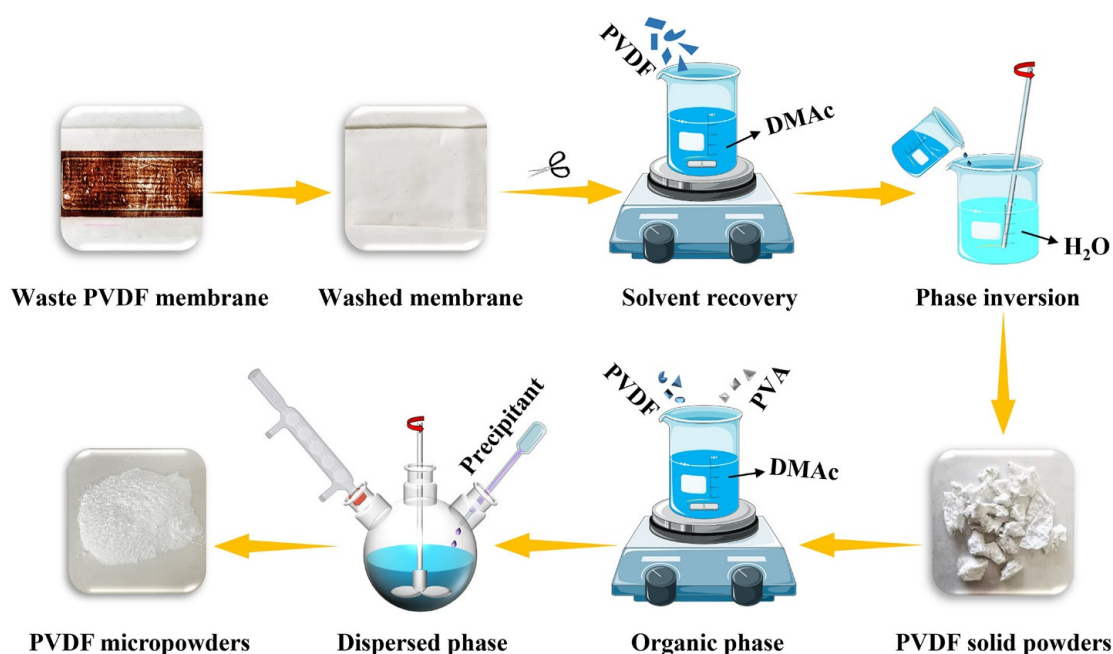


**Figure 13.** Synthesis steps for recycling PVDF micropowders from a waste PVDF membrane [105], Copyright 2023, reprinted with permission from John Wiley and Sons.

## 5. Conclusions and Future Outlook

This review has delved into the concerning issue of PFAS chemicals, a class of synthetic compounds widely used in various industrial and consumer products. Special emphasis was given to the usage, impacts, regulations, and remediation of the harmful effects of PFAS in lubricants and lubricating systems. A comprehensive discussion of the chemical structure of PFAS, and its environmental persistence that makes it a “forever chemical”, was followed by analyzing the performance of PFAS in lubricating oils, greases, additives, coatings, and composites, along with their fundamental working principles. Human exposure pathways and potential health implications associated with PFAS exposure were reported, shedding light on the widespread contamination of water, air, and soil, emphasizing the global scale of this environmental challenge.

This review’s main points can be summarized below:

- PFAS has seen extensive use in several industries and applications thanks to their strong C–F bonds and nonpolar nature.
- Their properties make them highly effective and efficient performance enhancers in tribology and lubrication systems, reducing friction coefficients and wear rates.
- These same properties make them resistant to natural degradation and are known to cause many negative health effects through bioaccumulation and environmental contamination as it is transported across various interfaces.
- Rigorous worldwide regulations continue to be introduced around the world in an effort to curtail the use of PFAS as the problem garners more attention given their persistent nature and documented adverse health effects.
- Remediation strategies involve various accelerated degradation techniques and PFAS material recovery through recycling; however, sourcing and utilizing PFAS alternatives remains the most effective method to reduce the world’s PFAS footprint.

The diverse performance aspects of PFAS, particularly PTFE and PVDF, as well as its role in emerging technologies such as ionic liquids, extreme pressure additives, and EVs, underscore their popularity in tribological applications. While PFAS remains highly resistant to natural breakdown, progress in electrochemical and biodegradation methods shows promise towards efficiently converting PFAS with minimal pollution. Alternative materials to PFAS such as shorter fluoroalkyl chains and structures with ether linkages or chlorinated carbons instead of exclusively fluorinated carbons are possible components of a replacement strategy. The complexity of mitigating PFAS contamination while simultaneously seeking its replacement highlights the urgency for innovative, sustainable solutions. The end of PFAS has been heralded, and the race has begun for what comes next.

**Author Contributions:** Literature gathering: D.D., J.B., A.K. and M.H.K. Writing: D.D., J.B., A.K., M.H.K. and H.L. All authors have read and agreed to the published version of the manuscript.

**Funding:** This research received no external funding.

**Data Availability Statement:** Not applicable.

**Conflicts of Interest:** The authors declare no conflict of interest.

## Glossary

AF	Antifriction
AFM	Atomic Force Microscope
AOP	Advanced Oxidation Process
API	American Petroleum Institute
ATR-FTIR	Attenuated Total Reflection-Fourier Transform Infrared Spectroscopy
ATSDR	Agency for Toxic Substances and Disease Registry
AW	Antiwear
BEV	Battery Electric Vehicle
CFC	Chlorofluorocarbons

---

CNF	Carbon Nanofiber
CNR	Carbon Nanorod
COF	Coefficient of Friction
EC	Electrocoagulation
ECHA	European Chemicals Agency
EO	Electro-oxidation
EP	Extreme Pressure
EPA	Environmental Protection Agency
ESIMS/MS	Electrospray Negative Ionization-Tandem Mass Spectrometry
EV	Electric Vehicle
FCEV	Fuel Cell Electric Vehicle
FEC	Fluorobenzene/Fluoroethylene Carbonate
FEP	Fluorinated Ethylene Propylene
FFKM	Perfluoroelastomer
FKM	Fluoroelastomer
FKM-O	FKM in Lubricating Oil
FT	Fluorotelomer
FTAL	Fluorotelomer Aldehyde
FTCA	Fluorotelomer Carboxylic Acid
FTOH	Fluorotelomer Alcohol
FTUCA	Fluorotelomer Unsaturated Carboxylic Acid
FVMQ	Fluorosilicone
GnPs	Graphene Nanoplatelet
HEP	Hydrofluoroethers
HFP	Hexafluoropropylene
HFPO-TA	Hexafluoropropylene Oxide Trifluoroacetate
ICE	Internal Combustion Engine
IL	Ionic Liquid
L-B104	1-butyl-3-methylimidazolium Tetrafluoroborate
LD50	Lethal Dosage 50
L-F104	1-butyl-3-methylimidazolium Bis[(trifluoromethyl)sulfonyl]imide
LOAEL	Lower Observed Adverse Effects Level
L-P104	1-butyl-3-methylimidazolium Hexafluorophosphate
MAC	Multialkylated Cyclopentane
MAO	Microarc Oxidized
MEC	Microbial Electrolysis Cell
MEMS	Micro-electromechanical System
NEMS	Nano-electromechanical System
NL	Nanolubricant
NNN	Novel Non-fluorinated Polymer
NOAEL	No Observable Adverse Effects Level
NP	Nanoparticle
NT	Nanotube
OBS	Oligomeric Siloxanes
OPE	Organophosphate Ester
PAO	Polyalphaolefin
PASF	Perfluoroalkane Sulfonyl Fluoride
PCTFE	Polychlorotrifluoroethylene
PDA	Polydopamine
PFAA	Perfluoroalkyl Acid
PFAS	Per- and Polyfluoroalkyl Substance
PFBA	Perfluorobutanoic Acid
PFC	Perfluorinated Chemical
PFC	Photocatalytic Fuel Cell
PFCA	Perfluorocarboxylic Acid
PFHpA	Perfluoroheptanoic Acid
PFHxA	Perfluorohexanoic Acid
PFHxS	Perfluorohexanesulfonic Acid

PFOA	Perfluorooctanoic Acid
PFOS	Perfluorooctane Sulfonic Acid
PFOSA	Perfluorooctanesulfonamide
PFPE	Perfluoroalkyl Ether
PFPeA	Perfluorovaleric Acid
PFSA	Perfluorosulfonic Acid
PHA	Polyhydroxyalkanoate
PLC	Polymers-of-low-concern
PMMA	Polymethylmethacrylate
POP	Persistent Organic Pollutant
PSF	Polysulfone
PSIL	Phosphonium-based Ionic Liquid
PTFE	Polytetrafluoroethylene
PVDF	Polyvinylidene Fluoride
PVF	Polyvinyl Fluoride
ROS	Reactive Oxygen Species
SA	Slide Angle
TFE	Tetrafluoroethylene
TFE/P	Tetrafluoroethylene Propylene
T <sub>g</sub>	Glass Transition Temperature
TOP	Total Oxidizable Precursor
TPP	Tetraalkyl Phosphonium Perfluorosulfonate
UF <sub>6</sub>	Uranium Hexafluoride
UV	Ultraviolet
VDF	Vinylidene Fluoride
WCA	Water Contact Angle
WSD	Wear Scar Diameter
WWTP	Wastewater Treatment Plant

## References

- Buck, R.C.; Franklin, J.; Berger, U.; Conder, J.M.; Cousins, I.T.; De Voogt, P.; Jensen, A.A.; Kannan, K.; Mabury, S.A.; Van Leeuwen, S.P.J. Perfluoroalkyl and Polyfluoroalkyl Substances in the Environment: Terminology, Classification, and Origins. *Integr. Environ. Assess. Manag.* **2011**, *7*, 513–541. [[CrossRef](#)] [[PubMed](#)]
- Brunn, H.; Arnold, G.; Körner, W.; Rippen, G.; Steinhäuser, K.G.; Valentin, I. PFAS: Forever Chemicals—Persistent, Bioaccumulative and Mobile. Reviewing the Status and the Need for Their Phase out and Remediation of Contaminated Sites. *Environ. Sci. Eur.* **2023**, *35*, 20. [[CrossRef](#)]
- Renfrew, D.; Pearson, T.W. The Social Life of the “Forever Chemical” PFAS Pollution Legacies and Toxic Events. *Environ. Soc. Adv. Res.* **2021**, *12*, 146–163. [[CrossRef](#)]
- Miner, K.R.; Clifford, H.; Taruscio, T.; Potocki, M.; Solomon, G.; Ritari, M.; Napper, I.E.; Gajurel, A.P.; Mayewski, P.A. Deposition of PFAS ‘Forever Chemicals’ on Mt. Everest. *Sci. Total Environ.* **2021**, *759*, 144421. [[CrossRef](#)] [[PubMed](#)]
- Okazoe, T. Overview on the History of Organofluorine Chemistry from the Viewpoint of Material Industry. *Proc. Jpn. Acad. Ser. B Phys. Biol. Sci.* **2009**, *85*, 276–289. [[CrossRef](#)] [[PubMed](#)]
- Kuwahara, T. Metal-Fluorocarbon Based Energetic Materials. *Propellants Explos. Pyrotech.* **2012**, *37*, 373. [[CrossRef](#)]
- Plunkett, R.J. Tetrafluoroethylene Polymers. U.S. Patent 2,230,654, 4 February 1941.
- Gaines, L.G.T. Historical and Current Usage of Per- and Polyfluoroalkyl Substances (PFAS): A Literature Review. *Am. J. Ind. Med.* **2023**, *66*, 353–378. [[CrossRef](#)] [[PubMed](#)]
- Glüge, J.; Scheringer, M.; Cousins, I.T.; Dewitt, J.C.; Goldenman, G.; Herzke, D.; Lohmann, R.; Ng, C.A.; Trier, X.; Wang, Z. An Overview of the Uses of Per- And Polyfluoroalkyl Substances (PFAS). *Environ. Sci. Process. Impacts* **2020**, *22*, 2345–2373. [[CrossRef](#)] [[PubMed](#)]
- Yeo, S.M.; Polycarpou, A.A. Tribological Performance of PTFE- and PEEK-Based Coatings under Oil-Less Compressor Conditions. *Wear* **2012**, *296*, 638–647. [[CrossRef](#)]
- Dubey, M.K.; Bijwe, J.; Ramakumar, S.S.V. Nano-PTFE: New Entrant as a Very Promising EP Additive. *Tribol. Int.* **2015**, *87*, 121–131. [[CrossRef](#)]
- Zheng, Q.; Chhattal, M.; Bai, C.; Zheng, Z.; Qiao, D.; Gong, Z.; Zhang, J. Superlubricity of PTFE Triggered by Green Ionic Liquids. *Appl. Surf. Sci.* **2023**, *614*, 156241. [[CrossRef](#)]
- Fan, M.; Jin, Y.; Han, Y.; Ma, L.; Li, W.; Lu, Y.; Zhou, F.; Liu, W. The Effect of Chemical Structure on the Tribological Performance of Perfluorosulfonate ILs as Lubricants for Ti-6Al-4V Tribopairs. *J. Mol. Liq.* **2021**, *321*, 114286. [[CrossRef](#)]
- Rico, E.F.; Minondo, I.; Cuervo, D.G. The Effectiveness of PTFE Nanoparticle Powder as an EP Additive to Mineral Base Oils. *Wear* **2007**, *262*, 1399–1406. [[CrossRef](#)]

15. Wang, Z.; Wu, L.; Qi, Y.; Cai, W.; Jiang, Z. Self-Lubricating Al<sub>2</sub>O<sub>3</sub>/PTFE Composite Coating Formation on Surface of Aluminium Alloy. *Surf. Coat. Technol.* **2010**, *204*, 3315–3318. [[CrossRef](#)]
16. Li, W.; Wang, Y.; Kannan, K. Occurrence, Distribution and Human Exposure to 20 Organophosphate Esters in Air, Soil, Pine Needles, River Water, and Dust Samples Collected around an Airport in New York State, United States. *Environ. Int.* **2019**, *131*, 105054. [[CrossRef](#)] [[PubMed](#)]
17. Le Magueresse-Battistoni, B.; Labaronne, E.; Vidal, H.; Naville, D. Endocrine Disrupting Chemicals in Mixture and Obesity, Diabetes and Related Metabolic Disorders. *World J. Biol. Chem.* **2017**, *8*, 108–119. [[CrossRef](#)] [[PubMed](#)]
18. *USA Lubricants Market Report 2018*; Research and Markets: Dublin, Ireland, 2019.
19. Wang, Y.; Munir, U.; Huang, Q. Occurrence of Per- and Polyfluoroalkyl Substances (PFAS) in Soil: Sources, Fate, and Remediation. *Soil Environ. Health* **2023**, *1*, 100004. [[CrossRef](#)]
20. Su, A.; Rajan, K. A Database Framework for Rapid Screening of Structure-Function Relationships in PFAS Chemistry. *Sci. Data* **2021**, *8*, 14. [[CrossRef](#)] [[PubMed](#)]
21. Frömel, T.; Knepper, T.P. Biodegradation of Fluorinated Alkyl Substances. *Rev. Environ. Contam. Toxicol.* **2010**, *208*, 161–177. [[CrossRef](#)] [[PubMed](#)]
22. Shahsavari, E.; Rouch, D.; Khudur, L.S.; Thomas, D.; Aburto-Medina, A.; Ball, A.S. Challenges and Current Status of the Biological Treatment of PFAS-Contaminated Soils. *Front. Bioeng. Biotechnol.* **2021**, *8*, 602040. [[CrossRef](#)] [[PubMed](#)]
23. Berhanu, A.; Mutanda, I.; Taolin, J.; Qaria, M.A.; Yang, B.; Zhu, D. A Review of Microbial Degradation of Per- and Polyfluoroalkyl Substances (PFAS): Biotransformation Routes and Enzymes. *Sci. Total Environ.* **2023**, *859*, 160010. [[CrossRef](#)] [[PubMed](#)]
24. Park, M.; Wu, S.; Lopez, I.J.; Chang, J.Y.; Karanfil, T.; Snyder, S.A. Adsorption of Perfluoroalkyl Substances (PFAS) in Groundwater by Granular Activated Carbons: Roles of Hydrophobicity of PFAS and Carbon Characteristics. *Water Res.* **2020**, *170*, 115364. [[CrossRef](#)] [[PubMed](#)]
25. Cai, W.; Navarro, D.A.; Du, J.; Ying, G.; Yang, B.; McLaughlin, M.J.; Kookana, R.S. Increasing Ionic Strength and Valency of Cations Enhance Sorption through Hydrophobic Interactions of PFAS with Soil Surfaces. *Sci. Total Environ.* **2022**, *817*, 152975. [[CrossRef](#)] [[PubMed](#)]
26. Verma, S.; Lee, T.; Sahle-Demessie, E.; Ateia, M.; Nadagouda, M.N. Recent Advances on PFAS Degradation via Thermal and Nonthermal Methods. *Chem. Eng. J. Adv.* **2023**, *13*, 100421. [[CrossRef](#)] [[PubMed](#)]
27. Cui, J.; Gao, P.; Deng, Y. Destruction of Per- and Polyfluoroalkyl Substances (PFAS) with Advanced Reduction Processes (ARPs): A Critical Review. *Environ. Sci. Technol.* **2020**, *54*, 3752–3766. [[CrossRef](#)] [[PubMed](#)]
28. Meegoda, J.N.; Kewalramani, J.A.; Li, B.; Marsh, R.W. A Review of the Applications, Environmental Release, and Remediation Technologies of per- and Polyfluoroalkyl Substances. *Int. J. Environ. Res. Public Health* **2020**, *17*, 8117. [[CrossRef](#)] [[PubMed](#)]
29. Wang, Z.; Ma, T. Lubricating Performance of Polytetrafluoroethylene Hybrid Fabric Composites with Removed Thermosetting Resin at Cryogenic Temperatures. *J. Appl. Polym. Sci.* **2023**, *140*, e53935. [[CrossRef](#)]
30. Liu, S.B.; Gong, H.; Qian, Y.; Zhao, J.B.; Ye, H.; Zhang, Z. The Friction and Wear Performance of Polytetrafluoroethylene Coating Reinforced with Modified Graphene. *Mater. Today Commun.* **2022**, *31*, 103448. [[CrossRef](#)]
31. Sun, W.; Liu, X.; Liu, K.; Xu, J.; Lu, Y.; Ye, J. Mechanochemical Functionality of Graphene Additives in Ultralow Wear Polytetrafluoroethylene Composites. *Carbon* **2021**, *184*, 312–321. [[CrossRef](#)]
32. Wang, Y.; Bai, Y. The Functionalization of Fluoroelastomers: Approaches, Properties, and Applications. *RSC Adv.* **2016**, *6*, 53730–53748. [[CrossRef](#)]
33. Améduri, B.; Boutevin, B.; Kostov, G. Fluoroelastomers: Synthesis, Properties and Applications. *Prog. Polym. Sci.* **2001**, *26*, 105–187. [[CrossRef](#)]
34. Li, F.; Duan, J.; Tian, S.; Ji, H.; Zhu, Y.; Wei, Z.; Zhao, D. Short-Chain per- and Polyfluoroalkyl Substances in Aquatic Systems: Occurrence, Impacts and Treatment. *Chem. Eng. J.* **2020**, *380*, 122506. [[CrossRef](#)]
35. Ohno, N.; Rahman, M.D.Z.; Syusuke Yamada; Komiya, H. Effect of Perfluoropolyether Fluids on Life of Thrust Ball Bearings. *Tribol. Trans.* **2009**, *52*, 492–500. [[CrossRef](#)]
36. Liang, J.; Helmick, L.S. Tribochemistry of a Pfpae Fluid on M-50 Surfaces by Ftir Spectroscopy. *Tribol. Trans.* **1996**, *39*, 705–709. [[CrossRef](#)]
37. Lin, A.Y.C.; Panchangam, S.C.; Lo, C.C. The Impact of Semiconductor, Electronics and Optoelectronic Industries on Downstream Perfluorinated Chemical Contamination in Taiwanese Rivers. *Environ. Pollut.* **2009**, *157*, 1365–1372. [[CrossRef](#)]
38. Pozo, K.; Moreira, L.B.; Karaskova, P.; Přibylková, P.; Klánová, J.; de Carvalho, M.U.; Maranhão, L.A.; de Souza Abessa, D.M. Using Large Amounts of Firefighting Foams Releases Per- and Polyfluoroalkyl Substances (PFAS) into Estuarine Environments: A Baseline Study in Latin America. *Mar. Pollut. Bull.* **2022**, *182*, 113938. [[CrossRef](#)] [[PubMed](#)]
39. Dauchy, X.; Boiteux, V.; Bach, C.; Rosin, C.; Munoz, J.F. Per- and Polyfluoroalkyl Substances in Firefighting Foam Concentrates and Water Samples Collected near Sites Impacted by the Use of These Foams. *Chemosphere* **2017**, *183*, 53–61. [[CrossRef](#)] [[PubMed](#)]
40. Alsmeyer, Y.W.; Childs, W.V.; Flynn, R.M.; Moore, G.G.I.; Smeltzer, J.C. *Electrochemical Fluorination and Its Applications*. In *Organofluorine Chemistry*; Springer: Boston, MA, USA, 1994.
41. Ebnesajjad, S. Synthesis and Properties of Monomers of Thermoplastic Fluoropolymers. In *Technology of Fluoropolymers*; CRC Press: Boca Raton, FL, USA, 2023.
42. Dhanumalayan, E.; Joshi, G.M. Performance Properties and Applications of Polytetrafluoroethylene (PTFE)—A Review. *Adv. Compos. Hybrid Mater.* **2018**, *1*, 247–268. [[CrossRef](#)]

43. Nishioka, A.; Matsumae, K.; Watanabe, M.; Tajima, M.; Owaki, M. Effects of Gamma Radiation on Some Physical Properties of Polytetrafluoroethylene Resin. *J. Appl. Polym. Sci.* **1959**, *2*, 114–119. [[CrossRef](#)]
44. Ariawan, A.B.; Ebnesajjad, S.; Hatzikiriakos, S.G. Preforming Behavior of Polytetrafluoroethylene Paste. *Powder Technol.* **2001**, *121*, 249–258. [[CrossRef](#)]
45. Yan, L.; Chao, M.; Xiao, J.; Gao, L.; Wießner, S. Study on Preparation of BaSO<sub>4</sub>-Containing Polytetrafluoroethylene Granular Powder. *Adv. Polym. Technol.* **2017**, *36*, 418–423. [[CrossRef](#)]
46. Puts, G.J.; Crouse, P.; Ameduri, B.M. Polytetrafluoroethylene: Synthesis and Characterization of the Original Extreme Polymer. *Chem. Rev.* **2019**, *119*, 1763–1805. [[CrossRef](#)] [[PubMed](#)]
47. Aderikha, V.N.; Krasnov, A.P.; Naumkin, A.V.; Shapovalov, V.A. Effects of Ultrasound Treatment of Expanded Graphite (EG) on the Sliding Friction, Wear Resistance, and Related Properties of PTFE-Based Composites Containing EG. *Wear* **2017**, *386–387*, 63–71. [[CrossRef](#)]
48. Kirillina, I.V.; Nikiforov, L.A.; Okhlopkova, A.A.; Sleptsova, S.A.; Yoon, C.; Cho, J.H. Nanocomposites Based on Polytetrafluoroethylene and Ultrahigh Molecular Weight Polyethylene: A Brief Review. *Bull. Korean Chem. Soc.* **2014**, *35*, 3411–3420. [[CrossRef](#)]
49. Huang, A.; Peng, X.; Turng, L.S. In-Situ Fibrillated Polytetrafluoroethylene (PTFE) in Thermoplastic Polyurethane (TPU) via Melt Blending: Effect on Rheological Behavior, Mechanical Properties, and Microcellular Foamability. *Polymer* **2018**, *134*, 263–274. [[CrossRef](#)]
50. Yin, Z.; Tian, B.; Zhu, Q.; Duan, C. Characterization and Application of PVDF and Its Copolymer Films Prepared by Spin-Coating and Langmuir-Blodgett Method. *Polymers* **2019**, *11*, 2033. [[CrossRef](#)] [[PubMed](#)]
51. Nguyen, A.N.; Solard, J.; Nong, H.T.T.; Ben Osman, C.; Gomez, A.; Bockelée, V.; Tencé-Girault, S.; Schoenstein, F.; Simón-Sorbed, M.; Carrillo, A.E.; et al. Spin Coating and Micro-Patterning Optimization of Composite Thin Films Based on PVDF. *Materials* **2020**, *13*, 1342. [[CrossRef](#)]
52. Cozza, E.S.; Monticelli, O.; Marsano, E.; Cebe, P. On the Electrospinning of PVDF: Influence of the Experimental Conditions on the Nanofiber Properties. *Polym. Int.* **2013**, *62*, 41–48. [[CrossRef](#)]
53. He, Z.; Rault, F.; Lewandowski, M.; Mohsenzadeh, E.; Salaün, F. Electrospun PVDF Nanofibers for Piezoelectric Applications: A Review of the Influence of Electrospinning Parameters on the  $\beta$  Phase and Crystallinity Enhancement. *Polymers* **2021**, *13*, 174. [[CrossRef](#)] [[PubMed](#)]
54. Kalimuldina, G.; Turdakyn, N.; Abay, I.; Medeubayev, A.; Nurpeissova, A.; Adair, D.; Bakenov, Z. A Review of Piezoelectric PvdF Film by Electrospinning and Its Applications. *Sensors* **2020**, *20*, 5214. [[CrossRef](#)] [[PubMed](#)]
55. Zhu, S.; Zhang, Y.; Li, Q.; Wei, L.; Guan, S. Influence of Polytetrafluoroethylene (PTFE) Content on Mechanical and Tribological Properties of Poly(Ether Ether Ketone)/PTFE Coatings Prepared by Electrostatic Powder Spraying Technique. *High Perform. Polym.* **2015**, *27*, 3–9. [[CrossRef](#)]
56. Weng, R.; Zhang, H.; Liu, X. Spray-Coating Process in Preparing PTFE-PPS Composite Super-Hydrophobic Coating. *AIP Adv.* **2014**, *4*, 031327. [[CrossRef](#)]
57. Leivo, E.; Wilenius, T.; Kinoshita, T.; Vuoristo, P.; Mäntylä, T. Properties of Thermally Sprayed Fluoropolymer PVDF, ECTFE, PFA and FEP Coatings. *Prog. Org. Coat.* **2004**, *49*, 69–73. [[CrossRef](#)]
58. Buck, R.C.; Murphy, P.M.; Pabon, M. Chemistry, Properties, and Uses of Commercial Fluorinated Surfactants. In *Polyfluorinated Chemicals and Transformation Products*; Springer: Berlin/Heidelberg, Germany, 2012.
59. Zhu, H.; Kannan, K. A Pilot Study of Per- and Polyfluoroalkyl Substances in Automotive Lubricant Oils from the United States. *Environ. Technol. Innov.* **2020**, *19*, 100943. [[CrossRef](#)]
60. Saleh, S.M.; Alminderej, F.M.; Mohamed, A.M.A. Superhydrophobic and Corrosion Behaviour of PVDF-CeO<sub>2</sub> Composite Coatings. *Materials* **2022**, *15*, 8674. [[CrossRef](#)] [[PubMed](#)]
61. Dong, M.; Hafezi, M.; Tong, Z.; Qin, L. Preparation and Oil Lubrication of Polyvinylidene Fluoride (PVDF) Nanospheres. *Mater. Res. Express* **2019**, *6*, 085093. [[CrossRef](#)]
62. Tansel, B. PFAS Use in Electronic Products and Exposure Risks during Handling and Processing of E-Waste: A Review. *J. Environ. Manag.* **2022**, *316*, 115291. [[CrossRef](#)] [[PubMed](#)]
63. Duncan, E.M.; Broderick, A.C.; Fuller, W.J.; Galloway, T.S.; Godfrey, M.H.; Hamann, M.; Limpus, C.J.; Lindeque, P.K.; Mayes, A.G.; Omeyer, L.C.M.; et al. Microplastic Ingestion Ubiquitous in Marine Turtles. *Glob. Chang. Biol.* **2019**, *25*, 744–752. [[CrossRef](#)]
64. Helmer, R.W.; Reeves, D.M.; Cassidy, D.P. Per- and Polyfluorinated Alkyl Substances (PFAS) Cycling within Michigan: Contaminated Sites, Landfills and Wastewater Treatment Plants. *Water Res.* **2022**, *210*, 117983. [[CrossRef](#)] [[PubMed](#)]
65. Wang, M.; Liu, K.; Yu, J.; Zhang, Q.; Zhang, Y.; Valix, M.; Tsang, D.C.W. Challenges in Recycling Spent Lithium-Ion Batteries: Spotlight on Polyvinylidene Fluoride Removal. *Glob. Chall.* **2023**, *7*, 2200237. [[CrossRef](#)] [[PubMed](#)]
66. Rajeevan, S.; John, S.; George, S.C. Polyvinylidene Fluoride: A Multifunctional Polymer in Supercapacitor Applications. *J. Power Sources* **2021**, *504*, 230037. [[CrossRef](#)]
67. Salam, M.A.R.B.A.; Rahman, M.A.; Kabir, M.H.; Alvarado, E.V.; Sadman, T.; Mahamud, R.; Cano, L.; Ashraf, A. Testing and Modeling of an in Situ Shear Exfoliated 2D Nanocomposite Coating Casing Material for the Suppression of Li-Ion Battery Fires in Electric Vehicles. *MRS Adv.* **2023**, *8*, 953–959. [[CrossRef](#)]
68. McMillan, R.; Slegel, H.; Shu, Z.X.; Wang, W. Fluoroethylene Carbonate Electrolyte and Its Use in Lithium Ion Batteries with Graphite Anodes. *J. Power Sources* **1999**, *81–82*, 20–26. [[CrossRef](#)]

69. Liu, M.; Zeng, Z.; Zhong, W.; Ge, Z.; Li, L.; Lei, S.; Wu, Q.; Zhang, H.; Cheng, S.; Xie, J. Non-Flammable Fluorobenzene-Diluted Highly Concentrated Electrolytes Enable High-Performance Li-Metal and Li-Ion Batteries. *J. Colloid Interface Sci.* **2022**, *619*, 399–406. [[CrossRef](#)] [[PubMed](#)]
70. Liu, F.; Yi, B.; Xing, D.; Yu, J.; Zhang, H. Nafion/PTFE Composite Membranes for Fuel Cell Applications. *J. Membr. Sci.* **2003**, *212*, 213–223. [[CrossRef](#)]
71. Benipal, N.; Qi, J.; Gentile, J.C.; Li, W. Direct Glycerol Fuel Cell with Polytetrafluoroethylene (PTFE) Thin Film Separator. *Renew. Energy* **2017**, *105*, 647–655. [[CrossRef](#)]
72. Scheel, K.-C.; Püschner, M. *PFAS in Automotive Technologies of the Future*; Verband der Automobilindustrie e.V.: Berlin, Germany, 2021.
73. Bulson, E.E.; Remucal, C.K.; Hicks, A.L. End-of-Life Circulation of PFAS in Metal Recycling Streams: A Sustainability-Focused Review. *Resour. Conserv. Recycl.* **2023**, *194*, 106978. [[CrossRef](#)]
74. Wickersham, L.C.; Mattila, J.M.; Krug, J.D.; Jackson, S.R.; Wallace, M.A.G.; Shields, E.P.; Halliday, H.; Li, E.Y.; Liberatore, H.K.; Fariior, S.; et al. Characterization of PFAS Air Emissions from Thermal Application of Fluoropolymer Dispersions on Fabrics. *J. Air Waste Manag. Assoc.* **2023**, *73*, 533–552. [[CrossRef](#)] [[PubMed](#)]
75. Nunez, E.E.; Gheisari, R.; Polycarpou, A.A. Tribology Review of Blended Bulk Polymers and Their Coatings for High-Load Bearing Applications. *Tribol. Int.* **2019**, *129*, 92–111. [[CrossRef](#)]
76. Kianfar, P.; Bongiovanni, R.; Ameduri, B.; Vitale, A. Electrospinning of Fluorinated Polymers: Current State of the Art on Processes and Applications. *Polym. Rev.* **2023**, *63*, 127–199. [[CrossRef](#)]
77. Ghosh, S.K.; Perez, G.; Goss, J.A.; Beckford, S.; Zou, M. Tribological Properties of PDA + PTFE Coating in Oil-Lubricated Condition. *Appl. Surf. Sci.* **2020**, *534*, 147627. [[CrossRef](#)]
78. Inderherbergh, J. Polyvinylidene Fluoride (PVDF) Appearance, General Properties and Processing. *Ferroelectrics* **1991**, *115*, 295–302. [[CrossRef](#)]
79. Dallaev, R.; Pisarenko, T.; Sobola, D.; Orudzhev, F.; Ramazanov, S.; Trčka, T. Brief Review of PVDF Properties and Applications Potential. *Polymers* **2022**, *14*, 4793. [[CrossRef](#)] [[PubMed](#)]
80. Xia, Z.; Wedel, A.; Danz, R. Charge Storage and Its Dynamics in Porous Polytetrafluoroethylene (PTFE) Film Electrets. *IEEE Trans. Dielectr. Electr. Insul.* **2003**, *10*, 102–108. [[CrossRef](#)]
81. Light, D.N.; Wilcox, J.R. Process Considerations in the Fabrication of Fluoropolymer Printed Circuit Boards. *IEEE Trans. Compon. Packag. Manuf. Technol. Part A* **1995**, *18*, 118–126. [[CrossRef](#)]
82. Catanese, J.; Cooke, D.; Maas, C.; Pruitt, L. Mechanical Properties of Medical Grade Expanded Polytetrafluoroethylene: The Effects of Internodal Distance, Density, and Displacement Rate. *J. Biomed. Mater. Res.* **1999**, *48*, 187–192. [[CrossRef](#)]
83. Teo, A.J.T.; Mishra, A.; Park, I.; Kim, Y.J.; Park, W.T.; Yoon, Y.J. Polymeric Biomaterials for Medical Implants and Devices. *ACS Biomater. Sci. Eng.* **2016**, *2*, 454–472. [[CrossRef](#)]
84. McCook, N.L.; Burris, D.L.; Dickrell, P.L.; Sawyer, W.G. Cryogenic Friction Behavior of PTFE Based Solid Lubricant Composites. *Tribol. Lett.* **2005**, *20*, 109–113. [[CrossRef](#)]
85. Thomas, P. The Use of Fluoropolymers for Non-Stick Cooking Utensils. *JOCCA Surf. Coat. Int.* **1998**, *81*, 604–609. [[CrossRef](#)]
86. Storgårds, E.; Simola, H.; Sjöberg, A.M.; Wirtanen, G. Hygiene of Gasket Materials Used in Food Processing Equipment Part 2: Aged Materials. *Food Bioprod. Process. Trans. Inst. Chem. Eng. Part C* **1999**, *77*, 146–155. [[CrossRef](#)]
87. Feng, S.; Zhong, Z.; Zhang, F.; Wang, Y.; Xing, W. Amphiphobic Polytetrafluoroethylene Membranes for Efficient Organic Aerosol Removal. *ACS Appl. Mater. Interfaces* **2016**, *8*, 8773–8781. [[CrossRef](#)] [[PubMed](#)]
88. Rodriguez-Lopez, J.; Alpuche-Aviles, M.A.; Bard, A.J. Selective Insulation with Poly(Tetrafluoroethylene) of Substrate Electrodes for Electrochemical Background Reduction in Scanning Electrochemical Microscopy. *Anal. Chem.* **2008**, *80*, 1813–1818. [[CrossRef](#)] [[PubMed](#)]
89. Peng, S.; Zhang, L.; Xie, G.; Guo, Y.; Si, L.; Luo, J. Friction and Wear Behavior of PTFE Coatings Modified with Poly (Methyl Methacrylate). *Compos. B Eng.* **2019**, *172*, 316–322. [[CrossRef](#)]
90. Miller, C.; Choudhury, D.; Zou, M. The Effects of Surface Roughness on the Durability of Polydopamine/PTFE Solid Lubricant Coatings on NiTiNOL 60. *Tribol. Trans.* **2019**, *62*, 919–929. [[CrossRef](#)]
91. Mohammadpourfazel, S.; Arash, S.; Ansari, A.; Yang, S.; Mallick, K.; Bagherzadeh, R. Future Prospects and Recent Developments of Polyvinylidene Fluoride (PVDF) Piezoelectric Polymer; Fabrication Methods, Structure, and Electro-Mechanical Properties. *RSC Adv.* **2023**, *13*, 370–387. [[CrossRef](#)] [[PubMed](#)]
92. Wang, S.; Shi, K.; Chai, B.; Qiao, S.; Huang, Z.; Jiang, P.; Huang, X. Core-Shell Structured Silk Fibroin/PVDF Piezoelectric Nanofibers for Energy Harvesting and Self-Powered Sensing. *Nano Mater. Sci.* **2022**, *4*, 126–132. [[CrossRef](#)]
93. Lee, H.; Bhushan, B. Nanotribology of Polyvinylidene Difluoride (PVDF) in the Presence of Electric Field. *J. Colloid Interface Sci.* **2011**, *360*, 777–784. [[CrossRef](#)] [[PubMed](#)]
94. Burkhart, M.; Wermelinger, J.; Setz, W.; Müller, D. Suitability of Polyvinylidene Fluoride (PVDF) Piping in Pharmaceutical Ultrapure Water Applications. *PDA J. Pharm. Sci. Technol.* **1996**, *50*, 246–251. [[PubMed](#)]
95. Liu, R.; Yuan, B.; Zhong, S.; Liu, J.; Dong, L.; Ji, Y.; Dong, Y.; Yang, C.; He, W. Poly(Vinylidene Fluoride) Separators for Next-generation Lithium Based Batteries. *Adv. Mater.* **2021**, *33*, 2308–2345. [[CrossRef](#)]
96. Cheng, Y.; Li, D. Numerical Analysis of Piezoelectric Signal of PVDF Membrane Flapping Wing in Flight. *IOP Conf. Ser. Mater. Sci. Eng.* **2020**, *774*, 012090. [[CrossRef](#)]

97. Ahmad, Z.; Prasad, A.; Prasad, K. A Comparative Approach to Predicting Effective Dielectric, Piezoelectric and Elastic Properties of PZT/PVDF Composites. *Phys. B Condens. Matter* **2009**, *404*, 3637–3644. [[CrossRef](#)]
98. Hussein, A.A.; Dawood, N.M.; Al-Kawaz, A.E. Corrosion Protection of 316L Stainless Steel by (PVDF/HA) Composite Coating Using a Spinning Coating Technique. *Bull. Pol. Acad. Sci. Tech. Sci.* **2021**, *69*, e136810. [[CrossRef](#)]
99. Remskar, M.; Jelenc, J.; Visic, B.; Varlec, A.; Cesarek, M.; Krzan, A. Friction Properties of Polyvinylidene Fluoride with Added MoS<sub>2</sub> Nanotubes. *Phys. Status Solidi A Appl. Mater. Sci.* **2013**, *210*, 2314–2319. [[CrossRef](#)]
100. Alazemi, A.A.; Dysart, A.D.; Shaffer, S.J.; Pol, V.G.; Stacke, L.E.; Sadeghi, F. Novel Tertiary Dry Solid Lubricant on Steel Surfaces Reduces Significant Friction and Wear under High Load Conditions. *Carbon* **2017**, *123*, 7–17. [[CrossRef](#)]
101. Clausi, M.; Grasselli, S.; Malchiodi, A.; Bayer, I.S. Thermally Conductive PVDF-Graphene Nanoplatelet (GnP) Coatings. *Appl. Surf. Sci.* **2020**, *529*, 147070. [[CrossRef](#)]
102. Park, M.S.; Sung, H.S.; Park, C.H.; Han, T.S.; Kim, J.H. High Tribology Performance of Poly(Vinylidene Fluoride) Composites Based on Three-Dimensional Mesoporous Magnesium Oxide Nanosheets. *Compos. B Eng.* **2019**, *163*, 224–235. [[CrossRef](#)]
103. Lee, J.H.; Park, M.S.; Lee, C.S.; Han, T.S.; Kim, J.H. Wear-Resistant Carbon Nanorod-Embedded Poly(Vinylidene Fluoride) Composites with Excellent Tribological Performance. *Compos. Part A Appl. Sci. Manuf.* **2020**, *129*, 105721. [[CrossRef](#)]
104. Wang, H.G.; Ren, J.F.; Jian, L.Q.; Pan, B.L.; Zhang, J.Y.; Yang, S.R. Friction and Wear Behavior of Polyamide 66/Poly(Vinylidene Fluoride) Blends. *J. Macromol. Sci. Part B Phys.* **2008**, *47*, 701–711. [[CrossRef](#)]
105. Liang, L.; Ma, Y.; Ji, X.; Ma, J.; Zhang, W.; Song, L. The Sustainable Recycling of Polyvinylidene Fluoride Membrane for Tribological Application. *J. Appl. Polym. Sci.* **2023**, *140*, e54287. [[CrossRef](#)]
106. Wang, H.; Liu, Z.; Wang, E.; Yuan, R.; Gao, D.; Zhang, X.; Zhu, Y. A Robust Superhydrophobic PVDF Composite Coating with Wear/Corrosion-Resistance Properties. *Appl. Surf. Sci.* **2015**, *332*, 518–524. [[CrossRef](#)]
107. Qu, M.; Yao, Y.; He, J.; Ma, X.; Feng, J.; Liu, S.; Hou, L.; Liu, X. Tribological Study of Polytetrafluoroethylene Lubricant Additives Filled with Cu Microparticles or SiO<sub>2</sub> Nanoparticles. *Tribol. Int.* **2017**, *110*, 57–65. [[CrossRef](#)]
108. Kumar Dubey, M.; Bijwe, J.; Ramakumar, S.S.V. PTFE Based Nano-Lubricants. *Wear* **2013**, *306*, 80–88. [[CrossRef](#)]
109. Li, X.; Lu, H.; Li, J.; Dong, G. Preparation and Lubricating Properties of Poly(Vinylidene-Fluoride) Particles Wrapped by Reduced Graphene Oxide. *Tribol. Int.* **2018**, *127*, 351–360. [[CrossRef](#)]
110. Zeng, Q. Superlow Friction and Diffusion Behaviors of a Steel-Related System in the Presence of Nano Lubricant Additive in PFPE Oil. *J. Adhes. Sci. Technol.* **2019**, *33*, 1001–1018. [[CrossRef](#)]
111. Fan, X.; Li, W.; Li, H.; Zhu, M.; Xia, Y.; Wang, J. Probing the Effect of Thickener on Tribological Properties of Lubricating Greases. *Tribol. Int.* **2018**, *118*, 128–139. [[CrossRef](#)]
112. Yang, J.; Li, X.; Liu, Y.; Wang, L. The Effect of Electron Irradiation on the Tribological Property of Perfluoropolyether Grease in Vacuum. *J. Fluor. Chem.* **2015**, *175*, 114–120. [[CrossRef](#)]
113. Gupta, T.C.S.M.; Kumar, A.; Prasad, B. Sustainable Lubrication: Low Molecular Weight PTFE Micro-Particles as Extreme Pressure Additives for Heavy Duty Grease Applications. *Ind. Lubr. Tribol.* **2021**, *73*, 1209–1218. [[CrossRef](#)]
114. Papay, A.G. Antiwear and Extreme-Pressure Additives in Lubricants. *Lubr. Sci.* **1998**, *10*, 209–224. [[CrossRef](#)]
115. Li, H.; Zhang, Y.; Li, C.; Zhou, Z.; Nie, X.; Chen, Y.; Cao, H.; Liu, B.; Zhang, N.; Said, Z.; et al. Extreme Pressure and Antiwear Additives for Lubricant: Academic Insights and Perspectives. *Int. J. Adv. Manuf. Technol.* **2022**, *120*, 1–27. [[CrossRef](#)]
116. Saini, V.; Bijwe, J.; Seth, S.; Ramakumar, S.S.V. Role of Base Oils in Developing Extreme Pressure Lubricants by Exploring Nano-PTFE Particles. *Tribol. Int.* **2020**, *143*, 106071. [[CrossRef](#)]
117. Gumprecht, W.H. Pr-143—A New Class of High-Temperature Fluids. *ASLE Trans.* **1966**, *9*, 24–30. [[CrossRef](#)]
118. Caporiccio, G.; Flabbi, L.; Marchionni, G.; Viola, G.T. The Properties and Applications of Perfluoropolyether Lubricants. *J. Synth. Lubr.* **1989**, *6*, 133–149. [[CrossRef](#)]
119. Snyder, C.E.; Gschwender, L.J. Fluoropolymers in Fluid and Lubricant Applications. *Ind. Eng. Chem. Prod. Res. Dev.* **1983**, *22*, 383–386. [[CrossRef](#)]
120. Nyberg, E.; Schneidhofer, C.; Pizarova, L.; Dörr, N.; Minami, I. Ionic Liquids as Performance Ingredients in Space Lubricants. *Molecules* **2021**, *26*, 1013. [[CrossRef](#)]
121. Jung, Y.; Yeo, C. Mechano-Chemical Properties and Tribological Performance of Thin Perfluoropolyether (PFPE) Lubricant Film under Environmental Contaminants. *Lubricants* **2023**, *11*, 306. [[CrossRef](#)]
122. Gleirscher, M.; Wolfberger, A.; Schlögl, S.; Holyńska, M.; Hausberger, A. Accelerated Thermo-Catalytic Degradation of Perfluoropolyether (PFPE) Lubricants for Space Applications. *Lubricants* **2023**, *11*, 81. [[CrossRef](#)]
123. Tao, Z.; Bhushan, B. Bonding, Degradation, and Environmental Effects on Novel Perfluoropolyether Lubricants. *Wear* **2005**, *259*, 1352–1361. [[CrossRef](#)]
124. Wolfberger, A.; Hausberger, A.; Schlögl, S.; Holyńska, M. Assessment of the Chemical Degradation of PFPE Lubricants and Greases for Space Applications: Implications for Long-Term on-Ground Storage. *CEAS Space J.* **2021**, *13*, 377–388. [[CrossRef](#)]
125. Sinha, S.K.; Kawaguchi, M.; Kato, T.; Kennedy, F.E. Wear Durability Studies of Ultra-Thin Perfluoropolyether Lubricant on Magnetic Hard Disks. *Tribol. Int.* **2003**, *36*, 217–225. [[CrossRef](#)]
126. He, Y.; Fujikawa, Y.; Zhang, H.; Fukuzawa, K.; Mitsuya, Y. Evaluations of Tribological Characteristics of PFPE Lubricants on DLC Surfaces of Magnetic Disks. *Tribol. Lett.* **2007**, *27*, 1–11. [[CrossRef](#)]
127. Gow, G. Lubricating Grease. In *Chemistry and Technology of Lubricants*; Mortier, R.M., Fox, M.F., Orszulik, S.T., Eds.; Springer: Dordrecht, The Netherlands, 2010; pp. 411–432. ISBN 978-1-4020-8662-5.

128. Derosa, T.F.; Kaufman, B.J.; Sung, R.L.; Russo, J.M. Dissolution of Perfluoroalkyl Oligomers in Lubricating Oil for Enhancing Wear Resistance and Fuel Economy. *J. Appl. Polym. Sci.* **1994**, *51*, 1339–1346. [CrossRef]
129. Zhao, M.; Yao, Y.; Dong, X.; Baqar, M.; Fang, B.; Chen, H.; Sun, H. Nontarget Identification of Novel Per- and Polyfluoroalkyl Substances (PFAS) in Soils from an Oil Refinery in Southwestern China: A Combined Approach with TOP Assay. *Environ. Sci. Technol.* **2023**, *57*, 20194–20205. [CrossRef] [PubMed]
130. Jin, C.M.; Ye, C.; Phillips, B.S.; Zabinski, J.S.; Liu, X.; Liu, W.; Shreeve, J.M. Polyethylene Glycol Functionalized Dicationic Ionic Liquids with Alkyl or Polyfluoroalkyl Substituents as High Temperature Lubricants. *J. Mater. Chem.* **2006**, *16*, 1529–1535. [CrossRef]
131. Wang, B.; Moran, C.; Lin, D.; Tang, H.; Gage, E.; Li, L. Nanometer-Thick Fluorinated Ionic Liquid Films as Lubricants in Data-Storage Devices. *ACS Appl. Nano Mater.* **2019**, *2*, 5260–5265. [CrossRef]
132. Lertola, A.C.; Wang, B.; Li, L. Understanding the Friction of Nanometer-Thick Fluorinated Ionic Liquids. *Ind. Eng. Chem. Res.* **2018**, *57*, 11681–11685. [CrossRef]
133. Blanco, D.; González, R.; Viesca, J.L.; Fernández-González, A.; Bartolomé, M.; Hernández Battez, A. Antifriction and Antiwear Properties of an Ionic Liquid with Fluorine-Containing Anion Used as Lubricant Additive. *Tribol. Lett.* **2017**, *65*, 66. [CrossRef]
134. Fan, M.; Zhang, C.; Guo, Y.; Zhang, R.; Lin, L.; Yang, D.; Zhou, F.; Liu, W. An Investigation on the Friction and Wear Properties of Perfluorooctane Sulfonate Ionic Liquids. *Tribol. Lett.* **2016**, *63*, 11. [CrossRef]
135. Romanova, N.V.; Shafigullin, L.N.; Buyatova, S.G. Study of the Local and Imported Rubber Products Made from Fluoroelastomer. *IOP Conf. Ser. Mater. Sci. Eng.* **2021**, *1079*, 022027. [CrossRef]
136. Améduri, B. Fluoropolymers as Unique and Irreplaceable Materials: Challenges and Future Trends in These Specific Per or Poly-Fluoroalkyl Substances. *Molecules* **2023**, *28*, 7564. [CrossRef] [PubMed]
137. Kalfayan, S.H.; Mazzeo, A.A.; Silver, R.H. Long-Term Aging of Elastomers. Chemical Stress Relaxation of Fluorosilicone Rubber and Other Studies. *JPL Quart. Tech. Rev.* **1971**, *1*, 38–47.
138. Hull, D.; Eggers, R.; Wellner, S. *TFE/P Based Elastomers Expand Seal/Lubricant Compatibility*; SAE Technical Paper 920709; SAE International: Warrendale, PA, USA, 1992. [CrossRef]
139. Chen, Z.; Christensen, L.; Dahn, J.R. Comparison of PVDF and PVDF-TFE-P as Binders for Electrode Materials Showing Large Volume Changes in Lithium-Ion Batteries. *J. Electrochem. Soc.* **2003**, *150*, A1073–A1078. [CrossRef]
140. Akhlaghi, S.; Pourrahimi, A.M.; Sjöstedt, C.; Bellander, M.; Hedenqvist, M.S.; Gedde, U.W. Degradation of Fluoroelastomers in Rapeseed Biodiesel at Different Oxygen Concentrations. *Polym. Degrad. Stab.* **2017**, *136*, 10–19. [CrossRef]
141. Wu, F.; Chen, B.; Pan, M. Degradation of the Sealing Silicone Rubbers in a Proton Exchange Membrane Fuel Cell at Cold Start Conditions. *Int. J. Electrochem. Sci.* **2020**, *15*, 3013–3028. [CrossRef]
142. Wang, S.; Wang, C.; He, A. Insights into the Effects of High-Temperature Lubricating Oils on the Aging Behavior and Degradation Mechanism of Fluoroelastomers. *Polym. Eng. Sci.* **2023**, *63*, 2371–2384. [CrossRef]
143. Wang, Q.L.; Pei, J.K.; Li, G.; He, X.; Niu, Y.H.; Li, G.X. Accelerated Aging Behaviors and Mechanism of Fluoroelastomer in Lubricating Oil Medium. *Chin. J. Polym. Sci. (Engl. Ed.)* **2020**, *38*, 853–866. [CrossRef]
144. Nowak, P.; Kucharska, K.; Kamiński, M. Ecological and Health Effects of Lubricant Oils Emitted into the Environment. *Int. J. Environ. Res. Public Health* **2019**, *16*, 3002. [CrossRef]
145. Diphare, M.J.; Pilusa, J.; Muzenda, E.; Mollagee, M. A Review of Waste Lubricating Grease Management. In Proceedings of the 2nd International Conference on Environment, Agriculture and Food Sciences (ICEAFS'2013), Kuala Lumpur, Malaysia, 6–7 May 2013; Available online: <https://api.semanticscholar.org/CorpusID:38915437> (accessed on 22 January 2024).
146. Brusseau, M.L.; Anderson, R.H.; Guo, B. PFAS Concentrations in Soils: Background Levels versus Contaminated Sites. *Sci. Total. Environ.* **2020**, *740*, 140017. [CrossRef] [PubMed]
147. Siddiqui, S.A.; Singh, S.; Bahmid, N.A.; Shyu, D.J.H.; Domínguez, R.; Lorenzo, J.M.; Pereira, J.A.M.; Câmara, J.S. Polystyrene Microplastic Particles in the Food Chain: Characteristics and Toxicity. A Review. *Sci. Total. Environ.* **2023**, *892*, 164531. [CrossRef] [PubMed]
148. Smalling, K.L.; Romanok, K.M.; Bradley, P.M.; Morriss, M.C.; Gray, J.L.; Kanagy, L.K.; Gordon, S.E.; Williams, B.M.; Breitmeyer, S.E.; Jones, D.K.; et al. Per- and Polyfluoroalkyl Substances (PFAS) in United States Tapwater: Comparison of Underserved Private-Well and Public-Supply Exposures and Associated Health Implications. *Environ. Int.* **2023**, *178*, 108033. [CrossRef] [PubMed]
149. MDH. *MDH Evaluation of Point-of-Use Water Treatment Devices for Perfluorochemical Removal*; Minnesota Department of Health: St. Paul, MN, USA, 2008.
150. Wang, P.; Zhang, M.; Li, Q.; Lu, Y. Atmospheric Diffusion of Perfluoroalkyl Acids Emitted from Fluorochemical Industry and Its Associated Health Risks. *Environ. Int.* **2021**, *146*, 106247. [CrossRef] [PubMed]
151. Schlummer, M.; Sölch, C.; Meisel, T.; Still, M.; Gruber, L.; Wolz, G. Emission of Perfluoroalkyl Carboxylic Acids (PFCA) from Heated Surfaces Made of Polytetrafluoroethylene (PTFE) Applied in Food Contact Materials and Consumer Products. *Chemosphere* **2015**, *129*, 46–53. [CrossRef] [PubMed]
152. Dalahmeh, S.; Tirgani, S.; Komakech, A.J.; Niwagaba, C.B.; Ahrens, L. Per- and Polyfluoroalkyl Substances (PFASs) in Water, Soil and Plants in Wetlands and Agricultural Areas in Kampala, Uganda. *Sci. Total. Environ.* **2018**, *631–632*, 660–667. [CrossRef] [PubMed]
153. Radulovic, L.L.; Wojcinski, Z.W. PTFE (Polytetrafluoroethylene; Teflon®). *Encycl. Toxicol.* **2024**, *7*, 1001–1006. [CrossRef]

154. Gaber, N.; Bero, L.; Woodruff, T.J. The Devil They Knew: Chemical Documents Analysis of Industry Influence on PFAS Science. *Ann. Glob. Health* **2023**, *89*, 37. [CrossRef]
155. Angela, K. *Oliver National Health and Nutrition Examination Survey (NHANES)*; National Center for Health Statistics: Hyattsville, MD, USA, 2022.
156. Agency for Toxic Substances and Disease Registry. ATSDR Toxicological Profiles. 2023. Available online: <https://www.atsdr.cdc.gov/toxprofiledocs/index.html> (accessed on 25 January 2024).
157. Boston University School of Public Health. Toxicology. 2019. Available online: <https://sphweb.bumc.bu.edu/otlt/MPH-Modules/PH717-QuantCore/PH717-Module2-ExposureAssessment/PH717-Module2-ExposureAssessment6.html> (accessed on 25 January 2024).
158. U.S. Department of Health and Human Services and Agency for Toxic Substances and Disease Registry. Toxicological Profile for Perfluoroalkyls. 2021. Available online: <https://www.atsdr.cdc.gov/toxprofiles/tp200.pdf> (accessed on 25 January 2024).
159. Alexander, B.H.; Olsen, G.W.; Burris, J.M.; Mandel, J.H.; Mandel, J.S. Mortality of Employees of a Perfluorooctanesulphonyl Fluoride Manufacturing Facility. *Occup. Environ. Med.* **2003**, *60*, 722–729. [CrossRef] [PubMed]
160. Steenland, K.; Tinker, S.; Shankar, A.; Ducatman, A. Association of Perfluorooctanoic Acid (PFOA) and Perfluorooctane Sulfonate (PFOS) with Uric Acid among Adults with Elevated Community Exposure to PFOA. *Environ. Health Perspect.* **2010**, *118*, 229–233. [CrossRef] [PubMed]
161. Consonni, D.; Straif, K.; Symons, J.M.; Tomenson, J.A.; Van Amelsvoort, L.G.P.M.; Smeuwenhoek, A.; Cherrie, J.W.; Bonetti, P.; Colombo, I.; Farrar, D.G.; et al. Cancer Risk among Tetrafluoroethylene Synthesis and Polymerization Workers. *Am. J. Epidemiol.* **2013**, *178*, 350–358. [CrossRef] [PubMed]
162. Grandjean, P.; Heilmann, C.; Weihe, P.; Nielsen, F.; Mogensen, U.B.; Budtz-Jørgensen, E. Serum Vaccine Antibody Concentrations in Adolescents Exposed to Perfluorinated Compounds. *Environ. Health Perspect.* **2017**, *125*, 077018. [CrossRef] [PubMed]
163. Marks, K.J.; Cutler, A.J.; Jeddy, Z.; Northstone, K.; Kato, K.; Hartman, T.J. Maternal Serum Concentrations of Perfluoroalkyl Substances and Birth Size in British Boys. *Int. J. Hyg. Environ. Health* **2019**, *222*, 889–895. [CrossRef]
164. Kang, J.S.; Ahn, T.G.; Park, J.W. Perfluorooctanoic Acid (PFOA) and Perfluorooctane Sulfonate (PFOS) Induce Different Modes of Action in Reproduction to Japanese Medaka (*Oryzias latipes*). *J. Hazard. Mater.* **2019**, *368*, 97–103. [CrossRef] [PubMed]
165. Huang, J.; Wang, Q.; Liu, S.; Lai, H.; Tu, W. Comparative Chronic Toxicities of PFOS and Its Novel Alternatives on the Immune System Associated with Intestinal Microbiota Dysbiosis in Adult Zebrafish. *J. Hazard. Mater.* **2022**, *425*, 127950. [CrossRef] [PubMed]
166. Roth, K.; Yang, Z.; Agarwal, M.; Liu, W.; Peng, Z.; Long, Z.; Birbeck, J.; Westrick, J.; Liu, W.; Petriello, M.C. Exposure to a Mixture of Legacy, Alternative, and Replacement per- and Polyfluoroalkyl Substances (PFAS) Results in Sex-Dependent Modulation of Cholesterol Metabolism and Liver Injury. *Environ. Int.* **2021**, *157*, 106843. [CrossRef] [PubMed]
167. Teunen, L.; Bervoets, L.; Belpaire, C.; De Jonge, M.; Groffen, T. PFAS Accumulation in Indigenous and Translocated Aquatic Organisms from Belgium, with Translation to Human and Ecological Health Risk. *Environ. Sci. Eur.* **2021**, *33*, 39. [CrossRef]
168. Yu, S.; Feng, W.R.; Liang, Z.M.; Zeng, X.Y.; Bloom, M.S.; Hu, G.C.; Zhou, Y.; Ou, Y.Q.; Chu, C.; Li, Q.Q.; et al. Perfluorooctane Sulfonate Alternatives and Metabolic Syndrome in Adults: New Evidence from the Isomers of C8 Health Project in China. *Environ. Pollut.* **2021**, *283*, 117078. [CrossRef] [PubMed]
169. Sunderland, E.M.; Hu, X.C.; Dassuncao, C.; Tokranov, A.K.; Wagner, C.C.; Allen, J.G. A Review of the Pathways of Human Exposure to Poly- and Perfluoroalkyl Substances (PFASs) and Present Understanding of Health Effects. *J. Expo. Sci. Environ. Epidemiol.* **2019**, *29*, 131–147. [CrossRef] [PubMed]
170. European Chemicals Agency. Per- and Polyfluoroalkyl Substances (PFAS)—ECHA. 2023. Available online: <https://echa.europa.eu/hot-topics/perfluoroalkyl-chemicals-pfas> (accessed on 25 January 2024).
171. Stockholm Convention. Stockholm Convention Overview. 2019. Available online: <https://chm.pops.int/TheConvention/Overview/tabid/3351/Default.aspx> (accessed on 25 January 2024).
172. Stockholm Convention. PFASs Listed under the Stockholm Convention. 2023. Available online: <https://chm.pops.int/Implementation/IndustrialPOPs/PFAS/Overview/tabid/5221/Default.aspx> (accessed on 25 January 2024).
173. United States Environmental Protection Agency. PFAS Strategic Roadmap: EPA’s Commitments to Action 2021–2024. 2021. Available online: [https://www.epa.gov/system/files/documents/2021-10/pfas-roadmap\\_final-508.pdf](https://www.epa.gov/system/files/documents/2021-10/pfas-roadmap_final-508.pdf) (accessed on 25 January 2024).
174. European Council. European Green Deal. 2023. Available online: <https://www.consilium.europa.eu/en/policies/green-deal/> (accessed on 25 January 2024).
175. European Council. European Green Deal: Commission Proposes Rules for Cleaner Air and Water. 2022. Available online: [https://ec.europa.eu/commission/presscorner/detail/en/IP\\_22\\_6278](https://ec.europa.eu/commission/presscorner/detail/en/IP_22_6278) (accessed on 25 January 2024).
176. Glüge, J.; London, R.; Cousins, I.T.; DeWitt, J.; Goldenman, G.; Herzke, D.; Lohmann, R.; Miller, M.; Ng, C.A.; Patton, S.; et al. Information Requirements under the Essential-Use Concept: PFAS Case Studies. *Environ. Sci. Technol.* **2021**, *56*, 6232–6242. [CrossRef] [PubMed]
177. Cousins, I.T.; Goldenman, G.; Herzke, D.; Lohmann, R.; Miller, M.; Ng, C.A.; Patton, S.; Scheringer, M.; Trier, X.; Vierke, L.; et al. The Concept of Essential Use for Determining When Uses of PFASs Can Be Phased Out. *Environ. Sci. Process. Impacts* **2019**, *21*, 1803–1815. [CrossRef] [PubMed]

178. Garcia-Segura, S.; Ocon, J.D.; Chong, M.N. Electrochemical Oxidation Remediation of Real Wastewater Effluents—A Review. *Process Saf. Environ. Prot.* **2018**, *113*, 48–67. [CrossRef]
179. Ganiyu, S.O.; Martínez-Huitle, C.A.; Oturan, M.A. Electrochemical Advanced Oxidation Processes for Wastewater Treatment: Advances in Formation and Detection of Reactive Species and Mechanisms. *Curr. Opin. Electrochem.* **2021**, *27*, 100678. [CrossRef]
180. Ganiyu, S.O.; Gamal El-Din, M. Insight into In-Situ Radical and Non-Radical Oxidative Degradation of Organic Compounds in Complex Real Matrix during Electrooxidation with Boron Doped Diamond Electrode: A Case Study of Oil Sands Process Water Treatment. *Appl. Catal. B Environ.* **2020**, *279*, 119366. [CrossRef]
181. Garcia-Rodriguez, O.; Mousset, E.; Olvera-Vargas, H.; Lefebvre, O. Electrochemical Treatment of Highly Concentrated Wastewater: A Review of Experimental and Modeling Approaches from Lab- to Full-Scale. *Crit. Rev. Environ. Sci. Technol.* **2022**, *52*, 240–309. [CrossRef]
182. Moreira, F.C.; Boaventura, R.A.R.; Brillas, E.; Vilar, V.J.P. Electrochemical Advanced Oxidation Processes: A Review on Their Application to Synthetic and Real Wastewaters. *Appl. Catal. B Environ.* **2017**, *202*, 217–261. [CrossRef]
183. Brillas, E.; Martínez-Huitle, C.A. Decontamination of Wastewaters Containing Synthetic Organic Dyes by Electrochemical Methods. An Updated Review. *Appl. Catal. B Environ.* **2015**, *166–167*, 603–643. [CrossRef]
184. Martínez-Huitle, C.A.; Ferro, S. Electrochemical Oxidation of Organic Pollutants for the Wastewater Treatment: Direct and Indirect Processes. *Chem. Soc. Rev.* **2006**, *35*, 1324–1340. [CrossRef] [PubMed]
185. Sivagami, K.; Sharma, P.; Karim, A.V.; Mohanakrishna, G.; Karthika, S.; Divyapriya, G.; Saravanathamizhan, R.; Kumar, A.N. Electrochemical-Based Approaches for the Treatment of Forever Chemicals: Removal of Perfluoroalkyl and Polyfluoroalkyl Substances (PFAS) from Wastewater. *Sci. Total. Environ.* **2023**, *861*, 160440. [CrossRef] [PubMed]
186. Nidheesh, P.V.; Kumar, A.; Syam Babu, D.; Scaria, J.; Suresh Kumar, M. Treatment of Mixed Industrial Wastewater by Electrocoagulation and Indirect Electrochemical Oxidation. *Chemosphere* **2020**, *251*, 126437. [CrossRef] [PubMed]
187. Ganiyu, S.O.; Martínez-Huitle, C.A.; Rodrigo, M.A. Renewable Energies Driven Electrochemical Wastewater/Soil Decontamination Technologies: A Critical Review of Fundamental Concepts and Applications. *Appl. Catal. B Environ.* **2020**, *270*, 118857. [CrossRef]
188. Cañizares, P.; Carmona, M.; Lobato, J.; Martínez, F.; Rodrigo, M.A. Electrodissolution of Aluminum Electrodes in Electrocoagulation Processes. *Ind. Eng. Chem. Res.* **2005**, *44*, 4178–4185. [CrossRef]
189. Kartikaningsih, D.; Shih, Y.J.; Huang, Y.H. Boron Removal from Boric Acid Wastewater by Electrocoagulation Using Aluminum as Sacrificial Anode. *Sustain. Environ. Res.* **2016**, *26*, 150–155. [CrossRef]
190. Kobya, M.; Can, O.T.; Bayramoglu, M. Treatment of Textile Wastewaters by Electrocoagulation Using Iron and Aluminum Electrodes. *J. Hazard. Mater.* **2003**, *100*, 163–178. [CrossRef] [PubMed]
191. Kabir, M.H.; Hossain, M.Z.; Jalil, M.A.; Ghosh, S.; Hossain, M.M.; Ali, M.A.; Khandaker, M.U.; Jana, D.; Rahman, M.M.; Hossain, M.K.; et al. The Efficacy of Rare-Earth Doped V<sub>2</sub>O<sub>5</sub> Photocatalyst for Removal of Pollutants from Industrial Wastewater. *Opt. Mater.* **2024**, *147*, 114724. [CrossRef]
192. Gar Alalm, M.; Boffito, D.C. Mechanisms and Pathways of PFAS Degradation by Advanced Oxidation and Reduction Processes: A Critical Review. *Chem. Eng. J.* **2022**, *450*, 138352. [CrossRef]
193. Rayaroth, M.P.; Aravind, U.K.; Aravindakumar, C.T. Degradation of Pharmaceuticals by Ultrasound-Based Advanced Oxidation Process. *Environ. Chem. Lett.* **2016**, *14*, 259–290. [CrossRef]
194. Sajjadi, B.; Raman, A.A.A.; Ibrahim, S. Influence of Ultrasound Power on Acoustic Streaming and Micro-Bubbles Formations in a Low Frequency Sono-Reactor: Mathematical and 3D Computational Simulation. *Ultrason. Sonochem.* **2015**, *24*, 193–203. [CrossRef] [PubMed]
195. Ince, N.H.; Tezcanli, G.; Belen, R.K.; Apikyan, G. Ultrasound as a Catalyzer of Aqueous Reaction Systems: The State of the Art and Environmental Applications. *Appl. Catal. B Environ.* **2001**, *29*, 167–176. [CrossRef]
196. Rayaroth, M.P.; Aravindakumar, C.T.; Shah, N.S.; Boczkaj, G. Advanced Oxidation Processes (AOPs) Based Wastewater Treatment—Unexpected Nitration Side Reactions—A Serious Environmental Issue: A Review. *Chem. Eng. J.* **2022**, *430*, 133002. [CrossRef]
197. Arias Espana, V.A.; Mallavarapu, M.; Naidu, R. Treatment Technologies for Aqueous Perfluorooctanesulfonate (PFOS) and Perfluorooctanoate (PFOA): A Critical Review with an Emphasis on Field Testing. *Environ. Technol. Innov.* **2015**, *4*, 168–181. [CrossRef]
198. Ciawi, E.; Rae, J.; Ashokkumar, M.; Grieser, F. Determination of Temperatures within Acoustically Generated Bubbles in Aqueous Solutions at Different Ultrasound Frequencies. *J. Phys. Chem. B* **2006**, *110*, 13656–13660. [CrossRef]
199. Hori, H.; Nagaoka, Y.; Yamamoto, A.; Sano, T.; Yamashita, N.; Taniyasu, S.; Kutsuna, S.; Osaka, I.; Arakawa, R. Efficient Decomposition of Environmentally Persistent Perfluorooctanesulfonate and Related Fluorochemicals Using Zerovalent Iron in Subcritical Water. *Environ. Sci. Technol.* **2006**, *40*, 1049–1054. [CrossRef]
200. Lee, Y.C.; Lo, S.L.; Chiueh, P.T.; Chang, D.G. Efficient Decomposition of Perfluorocarboxylic Acids in Aqueous Solution Using Microwave-Induced Persulfate. *Water Res.* **2009**, *43*, 2811–2816. [CrossRef] [PubMed]
201. Hori, H.; Nagaoka, Y.; Sano, T.; Kutsuna, S. Iron-Induced Decomposition of Perfluorohexanesulfonate in Sub- and Supercritical Water. *Chemosphere* **2008**, *70*, 800–806. [CrossRef]
202. Hori, H.; Murayama, M.; Sano, T.; Kutsuna, S. Decomposition of Perfluorinated Ion-Exchange Membrane to Fluoride Ions Using Zerovalent Metals in Subcritical Water. *Ind. Eng. Chem. Res.* **2010**, *49*, 464–471. [CrossRef]

203. Yi, L.B.; Chai, L.Y.; Xie, Y.; Peng, Q.J.; Peng, Q.Z. Isolation, Identification, and Degradation Performance of a PFOA-Degrading Strain. *Genet. Mol. Res.* **2016**, *15*, 235–246. [[CrossRef](#)] [[PubMed](#)]
204. Huang, S.; Jaffé, P.R. Defluorination of Perfluorooctanoic Acid (PFOA) and Perfluorooctane Sulfonate (PFOS) by *Acidimicrobium* Sp. Strain A6. *Environ. Sci. Technol.* **2019**, *53*, 11410–11419. [[CrossRef](#)] [[PubMed](#)]
205. Huang, S.; Sima, M.; Long, Y.; Messenger, C.; Jaffé, P.R. Anaerobic Degradation of Perfluorooctanoic Acid (PFOA) in Biosolids by *Acidimicrobium* sp. Strain A6. *J. Hazard. Mater.* **2022**, *424*, 127699. [[CrossRef](#)] [[PubMed](#)]
206. Ruiz-Urigüen, M.; Shuai, W.; Huang, S.; Jaffé, P.R. Biodegradation of PFOA in Microbial Electrolysis Cells by *Acidimicrobiaceae* sp. Strain A6. *Chemosphere* **2022**, *292*, 133506. [[CrossRef](#)] [[PubMed](#)]
207. Key, B.D.; Howell, R.D.; Criddle, C.S. Defluorination of Organofluorine Sulfur Compounds by *Pseudomonas* sp. Strain D2. *Environ. Sci. Technol.* **1998**, *32*, 2283–2287. [[CrossRef](#)]
208. Kwon, B.G.; Lim, H.J.; Na, S.H.; Choi, B.I.; Shin, D.S.; Chung, S.Y. Biodegradation of Perfluorooctanesulfonate (PFOS) as an Emerging Contaminant. *Chemosphere* **2014**, *109*, 221–225. [[CrossRef](#)] [[PubMed](#)]
209. Dinglasan, M.J.A.; Ye, Y.; Edwards, E.A.; Mabury, S.A. Fluorotelomer Alcohol Biodegradation Yields Poly- and Perfluorinated Acids. *Environ. Sci. Technol.* **2004**, *38*, 2857–2864. [[CrossRef](#)] [[PubMed](#)]
210. Kim, M.H.; Wang, N.; McDonald, T.; Chu, K.H. Biodefluorination and Biotransformation of Fluorotelomer Alcohols by Two Alkane-Degrading *Pseudomonas* Strains. *Biotechnol. Bioeng.* **2012**, *109*, 3041–3048. [[CrossRef](#)] [[PubMed](#)]
211. Wang, N.; Szostek, B.; Buck, R.C.; Folsom, P.W.; Sulecki, L.M.; Capka, V.; Berti, W.R.; Gannon, J.T. Fluorotelomer Alcohol Biodegradation—Direct Evidence That Perfluorinated Carbon Chains Breakdown. *Environ. Sci. Technol.* **2005**, *39*, 7516–7528. [[CrossRef](#)] [[PubMed](#)]
212. Wang, N.; Szostek, B.; Buck, R.C.; Folsom, P.W.; Sulecki, L.M.; Gannon, J.T. 8-2 Fluorotelomer Alcohol Aerobic Soil Biodegradation: Pathways, Metabolites, and Metabolite Yields. *Chemosphere* **2009**, *75*, 1089–1096. [[CrossRef](#)] [[PubMed](#)]
213. Li, F.; Su, Q.; Zhou, Z.; Liao, X.; Zou, J.; Yuan, B.; Sun, W. Anaerobic Biodegradation of 8:2 Fluorotelomer Alcohol in Anaerobic Activated Sludge: Metabolic Products and Pathways. *Chemosphere* **2018**, *200*, 124–132. [[CrossRef](#)] [[PubMed](#)]
214. Hamid, H.; Li, L.Y.; Grace, J.R. Aerobic Biotransformation of Fluorotelomer Compounds in Landfill Leachate-Sediment. *Sci. Total. Environ.* **2020**, *713*, 136547. [[CrossRef](#)] [[PubMed](#)]
215. Yu, X.; Takabe, Y.; Yamamoto, K.; Matsumura, C.; Nishimura, F. Biodegradation Property of 8:2 Fluorotelomer Alcohol (8:2 FTOH) under Aerobic/Anoxic/Anaerobic Conditions. *J. Water Environ. Technol.* **2016**, *14*, 177–190. [[CrossRef](#)]
216. Yu, Y.; Zhang, K.; Li, Z.; Ren, C.; Chen, J.; Lin, Y.H.; Liu, J.; Men, Y. Microbial Cleavage of C-F Bonds in Two C6Per- And Polyfluorinated Compounds via Reductive Defluorination. *Environ. Sci. Technol.* **2020**, *54*, 14393–14402. [[CrossRef](#)] [[PubMed](#)]
217. Yu, Y.; Che, S.; Ren, C.; Jin, B.; Tian, Z.; Liu, J.; Men, Y. Microbial Defluorination of Unsaturated Per- and Polyfluorinated Carboxylic Acids under Anaerobic and Aerobic Conditions: A Structure Specificity Study. *Environ. Sci. Technol.* **2022**, *56*, 4894–4904. [[CrossRef](#)] [[PubMed](#)]
218. Goldman, P. The Enzymatic Cleavage of The Carbon-Fluorine Bond in Fluoroacetate. *J. Biol. Chem.* **1965**, *240*, 3434–3438. [[CrossRef](#)] [[PubMed](#)]
219. Leong, L.E.X.; Denman, S.E.; Hugenholtz, P.; McSweeney, C.S. Amino Acid and Peptide Utilization Profiles of the Fluoroacetate-Degrading Bacterium *Synergistetes* Strain MFA1 Under Varying Conditions. *Microb. Ecol.* **2016**, *71*, 494–504. [[CrossRef](#)] [[PubMed](#)]
220. Leong, L.E.X.; Khan, S.; Davis, C.K.; Denman, S.E.; McSweeney, C.S. Fluoroacetate in Plants—A Review of Its Distribution, Toxicity to Livestock and Microbial Detoxification. *J. Anim. Sci. Biotechnol.* **2017**, *8*, 55. [[CrossRef](#)] [[PubMed](#)]
221. Murphy, C.D. Biodegradation and Biotransformation of Organofluorine Compounds. *Biotechnol. Lett.* **2010**, *32*, 351–359. [[CrossRef](#)] [[PubMed](#)]
222. Seong, H.J.; Kwon, S.W.; Seo, D.C.; Kim, J.H.; Jang, Y.S. Enzymatic Defluorination of Fluorinated Compounds. *Appl. Biol. Chem.* **2019**, *62*, 62. [[CrossRef](#)]
223. Li, Y.; Zhang, R.; Du, L.; Zhang, Q.; Wang, W. Catalytic Mechanism of C-F Bond Cleavage: Insights from QM/MM Analysis of Fluoroacetate Dehalogenase. *Catal. Sci. Technol.* **2016**, *6*, 73–80. [[CrossRef](#)]
224. Dickman, R.A.; Aga, D.S. A Review of Recent Studies on Toxicity, Sequestration, and Degradation of per- and Polyfluoroalkyl Substances (PFAS). *J. Hazard. Mater.* **2022**, *436*, 129120. [[CrossRef](#)] [[PubMed](#)]
225. Ateia, M.; Maroli, A.; Tharayil, N.; Karanfil, T. The Overlooked Short- and Ultrashort-Chain Poly- and Perfluorinated Substances: A Review. *Chemosphere* **2019**, *220*, 866–882. [[CrossRef](#)] [[PubMed](#)]
226. Mantripragada, S.; Obare, S.O.; Zhang, L. Addressing Short-Chain PFAS Contamination in Water with Nanofibrous Adsorbent/Filter Material from Electrospinning. *Acc. Chem. Res.* **2023**, *56*, 1271–1278. [[CrossRef](#)] [[PubMed](#)]
227. Talha, M.; Ma, Y.; Xu, M.; Wang, Q.; Lin, Y.; Kong, X. Recent Advancements in Corrosion Protection of Magnesium Alloys by Silane-Based Sol-Gel Coatings. *Ind. Eng. Chem. Res.* **2020**, *59*, 19840–19857. [[CrossRef](#)]
228. Chen, F.; Teniola, O.R.; Ogueri, K.S.; Laurencin, C.T. Recent Trends in the Development of Polyphosphazenes for Bio-Applications. *Regen. Eng. Transl. Med.* **2023**, *9*, 202–223. [[CrossRef](#)]
229. Ma, W.; Lopez, G.; Ameduri, B.; Takahara, A. Fluoropolymer Nanoparticles Prepared Using Trifluoropropene Telomer Based Fluorosurfactants. *Langmuir* **2020**, *36*, 1754–1760. [[CrossRef](#)] [[PubMed](#)]
230. Shimojima, A.; Liu, Z.; Ohsuna, T.; Terasaki, O.; Kuroda, K. Self-Assembly of Designed Oligomeric Siloxanes with Alkyl Chains into Silica-Based Hybrid Mesostructures. *J. Am. Chem. Soc.* **2005**, *127*, 14108–14116. [[CrossRef](#)] [[PubMed](#)]

231. Suresh Babu, D.; Mol, J.M.C.; Buijnsters, J.G. Experimental Insights into Anodic Oxidation of Hexafluoropropylene Oxide Dimer Acid (GenX) on Boron-Doped Diamond Anodes. *Chemosphere* **2022**, *288*, 132417. [[CrossRef](#)] [[PubMed](#)]
232. Bhutta, M.U.; Khan, Z.A. Friction and Wear Performance Analysis of Hydrofluoroether-7000 Refrigerant. *Tribol. Int.* **2019**, *139*, 36–54. [[CrossRef](#)]
233. Esmaeili, N.; Gray, E.M.A.; Webb, C.J. Non-Fluorinated Polymer Composite Proton Exchange Membranes for Fuel Cell Applications—A Review. *ChemPhysChem* **2019**, *20*, 2016–2053. [[CrossRef](#)] [[PubMed](#)]
234. Mehrpouya, M.; Vahabi, H.; Barletta, M.; Laheurte, P.; Langlois, V. Additive Manufacturing of Polyhydroxyalkanoates (PHAs) Biopolymers: Materials, Printing Techniques, and Applications. *Mater. Sci. Eng. C* **2021**, *127*, 112216. [[CrossRef](#)] [[PubMed](#)]
235. Nowak, T.; Mazela, B.; Olejnik, K.; Peplińska, B.; Perdoch, W. Starch-Silane Structure and Its Influence on the Hydrophobic Properties of Paper. *Molecules* **2022**, *27*, 3136. [[CrossRef](#)] [[PubMed](#)]
236. Albright, V.; Penarete-Acosta, D.; Stack, M.; Zheng, J.; Marin, A.; Hlushko, H.; Wang, H.; Jayaraman, A.; Andrianov, A.K.; Sukhishvili, S.A. Polyphosphazenes Enable Durable, Hemocompatible, Highly Efficient Antibacterial Coatings. *Biomaterials* **2021**, *268*, 120586. [[CrossRef](#)] [[PubMed](#)]
237. Peshoria, S.; Nandini, D.; Tanwar, R.K.; Narang, R. Short-Chain and Long-Chain Fluorosurfactants in Firefighting Foam: A Review. *Environ. Chem. Lett.* **2020**, *18*, 1277–1300. [[CrossRef](#)]
238. He, J.; Zhou, L.; Soucek, M.D.; Wollyung, K.M.; Wesdemiotis, C. UV-Curable Hybrid Coatings Based on Vinylfunctionized Siloxane Oligomer and Acrylated Polyester. *J. Appl. Polym. Sci.* **2007**, *105*, 2376–2386. [[CrossRef](#)]
239. Peng, B.X.; Li, F.; Mortimer, M.; Xiao, X.; Ni, Y.; Lei, Y.; Li, M.; Guo, L.H. Perfluorooctanoic Acid Alternatives Hexafluoropropylene Oxides Exert Male Reproductive Toxicity by Disrupting Blood-Testis Barrier. *Sci. Total. Environ.* **2022**, *846*, 157313. [[CrossRef](#)] [[PubMed](#)]
240. Vinš, V.; Aminian, A.; Celný, D.; Součková, M.; Klomfar, J.; Čenský, M.; Prokopová, O. Surface Tension and Density of Dielectric Heat Transfer Fluids of HFE Type-Experimental Data at 0.1 MPa and Modeling with PC-SAFT Equation of State and Density Gradient Theory. *Int. J. Refrig.* **2021**, *131*, 956–969. [[CrossRef](#)]
241. Ovaskainen, L.; Rodriguez-Meizoso, I.; Birkin, N.A.; Howdle, S.M.; Gedde, U.; Wågberg, L.; Turner, C. Towards Superhydrophobic Coatings Made by Non-Fluorinated Polymers Sprayed from a Supercritical Solution. *J. Supercrit. Fluids* **2013**, *77*, 134–141. [[CrossRef](#)]
242. Samrot, A.V.; Samanvitha, S.K.; Shobana, N.; Renitta, E.R.; Kumar, P.S.; Kumar, S.S.; Abirami, S.; Dhiva, S.; Bavanilatha, M.; Prakash, P.; et al. The Synthesis, Characterization and Applications of Polyhydroxyalkanoates (Phas) and Pha-Based Nanoparticles. *Polymers* **2021**, *13*, 3302. [[CrossRef](#)] [[PubMed](#)]
243. Richard, R. Thomas Fluorinated Surfactant. In *Chemistry and Technology of Surfactants*; Farn, R.J., Ed.; Wiley: Hoboken, NJ, USA, 2006; Volume 1, pp. 227–235.
244. Cirisano, F.; Ferrari, M. Superhydrophobicity and Durability in Recyclable Polymers Coating. *Sustainability* **2021**, *13*, 8244. [[CrossRef](#)]
245. Améduri, B.; Hori, H. Recycling and the End of Life Assessment of Fluoropolymers: Recent Developments, Challenges and Future Trends. *Chem. Soc. Rev.* **2023**, *52*, 4208–4247. [[CrossRef](#)] [[PubMed](#)]
246. pro-K Fluoropolymergroup. Recycling of Fluoropolymers. 2018. Available online: <https://www.pro-kunststoff.de/fachwissen/recycling-of-fluoropolymers.html> (accessed on 25 January 2024).

**Disclaimer/Publisher’s Note:** The statements, opinions and data contained in all publications are solely those of the individual author(s) and contributor(s) and not of MDPI and/or the editor(s). MDPI and/or the editor(s) disclaim responsibility for any injury to people or property resulting from any ideas, methods, instructions or products referred to in the content.